Development and Evolution of Cell Behavior and Interactions during *Danio* Pattern Formation

Emily Bain

A dissertation

Submitted in partial fulfillment of the

Requirements for the degree of

Doctor of Philosophy

University of Washington

2018

Reading Committee:

David Parichy, Chair

Keiko Torii

Jay Parrish

Program Authorized to Offer Degree:

Biology

University of Washington

Abstract

Development and Evolution of Cell Behavior and Interactions during *Danio* Pattern Formation

Emily Bain

Chair of the Supervisory Committee:
Professor David Parichy
Biology

Danio fishes offer a tractable system for elucidating mechanisms of pattern formation and how they evolve, as fishes in this genus display a diverse array of pigment patterns that arise from a common set of cell types. Zebrafish (*Danio rerio*) forms its adult pattern beginning with a primary interstripe of densely packed iridescent iridophores and yellow xanthophores, with dark stripes of black melanophores and loose iridophores forming dorsally and ventrally. Additional interstripes and stripes are then reiterated to yield the final adult pattern. Stripe formation requires positive and negative interactions between pigment cells and between pigment cells and their environment, but the specific cell behaviors underlying morphogenesis are just beginning to be understood. Here I use time-lapse imaging, cell marking, and other genetic approaches to identify new features of iridophore morphogenesis and differentiation in zebrafish and manipulative experiments to dissect iridophore behavior during pattern formation. Additionally, I explore how changes in pigment cell-cell communication and global hormonal signals have evolved in the closely related species, pearl danio, whose uniform pattern is in stark contrast to zebrafish stripes. Together these data advance our understanding of a rapidly

growing model of *Danio* pigment pattern formation and how the evolution of cellular interactions gives rise to the stunning diversity of adult form.

Acknowledgments

My sincerest gratitude to past and present members of the Parichy Lab for their support, encouragement, and scientific prowess. Thanks to Sarah, Larissa, Dae Seok, and Andy for being mentors when I needed one and fellow complainers the rest of the time. Thanks also to all the Bio grads and DBTGers for stimulating conversation and showcasing the breadth of cool science that we get to do. **Thank you, Dave, for the opportunity to do work I'm proud of and for giving me the fortitude to keep going even when science sucks.**

To Mom and David
Thank you. From the bottom of my heart, for everything.

To Jessica
Thanks for being the Amy to my Tina. That's all I can write down because everything else is too cheesy and stoopid and you'd make fun of me anyway…and my eyes are sweating.

To Kory, Stephanie, Rahn, Becky, RJ
Thanks for laughing at butt jokes and making Thursdays the best days.

To Steve, Norm, Dan, Robin, Lydia, McKenna
Thanks for making me a regular, and occasionally smart and rich.

To Peter
Thanks for making the darkest part of grad school a little brighter.

To Microsoft
Thanks for keeping Minesweeper installed on even the fanciest of computers since 1990.

Table of Contents

List of Figures

Introduction

Pattern and boundary formation are critical aspects of multicellular development. Patterning is important in the embryo to establish discrete domains and arrangments of different cell types that go on to form tissues and organs of the adult. These patterns exist from the level of gene expression, as in the pair rule genes of *Drosophila*, to complex tissues, as in the divisions between rhombomeres of vertebrates, compartmentalization in *Drosophila* imaginal disks, and lineage restrictions in the developing limb bud[1–5]. Whether occurring through classically envisaged morphogen gradients, cell-sorting or other mechanisms, pattern formation necessarily depends on the timing and location of cellular differentiation, migration, and proliferation[2,6–8]. Such behaviors do not end with embryogenesis: patterns must be maintained in the context of normal growth and re-established during wound healing and regeneration. In humans, defects in pattern maintenance can have severe consequences, most notably in cancer metastasis, when cells escape the primary tumor and colonize other locations, a phenomenon typically more dangerous than the initial tumor[9,10].

Perhaps the most striking example of pattern formation is body coloration. It is easily visible on the outside of an organism, is physiologically, evolutionarily, and ecologically relevant, and often genetically tractable for experimental manipulations. Pigmentation has been a target for artificial selection for centuries from the mouse fanciers of ancient China to pigeon aficionados showing their prized Scandaroon[11–13]. Pigment cells are derived from the neural crest, a transient embryonic cell population found only in vertebrates that is thought to be responsible for much of the phenotypic diversity across the subphylum[14]. In addition to pigment cells, peripheral nerves and glia, some cardiac tissue, and craniofacial bones and cartilage are all derivatives of the neural crest[15]. For example, the prodigious range of skull morphologies in domestic dog breeds, e.g., the squashed pug face or elongated greyhound muzzle, stem from differential deployment of neural crest cells during early development in ostensibly the same

species, *Canis familiaris*[16,17]. Within breeds, differences in coat color like brindled, black, and yellow of Labradors are linked to the regulation of pigment production in cells stemming from the neural crest[18].

Historic models of pigment pattern formation have been birds and mammals that contain a single pigment cell type, the melanocyte. These pigment producing cells synthesize brown/black eumelanin or red/brown pheomelanin and then transfer it to a secondary cell type such as the keratinocytes in a developing hair follicle or feather[19–21]. Conversely, poikilotherms, e.g., fish, amphibians, and reptiles, have evolved multiple pigment cell types that retain pigment after it is produced making them particularly amenable to cell-cell interaction studies as the naturally occurring pigment precludes the need for a genetically encoded cell marker.

Zebrafish, *Danio rerio*, have exploded in popularity as a biomedical model system with all the advantages thereof – sufficient genomic resources, a wealth of molecular tools and reagents, and emerging disease models to study human pathologies. The adult pigment pattern is deceptively simple comprising three to four dark stripes of black melanophores separated by lighter interstripes of yellow xanthophores. A third pigment cell, the iridescent iridophore, is found in two conformations along the flank. Superficial to melanophores in the stripe, adopting a “loose,” dendritic-like appearance, and “dense” in the interstripe region where they form a tightly packed, epithelial-like mat deep to the xanthophores[22]. These dense iridophores are the first adult pigment cell type to develop in the location of the primary interstripe spreading anterior to posterior in the middle of the flank during the larval-to-adult transition[23,24]. Black melanophores next appear broadly along the flank and coalesce into stripes on either side of the burgeoning interstripe. Yellow xanthophores then differentiate on top of the dense iridophores. This pattern is reiterated as new interstripes and stripes are added dorsally and ventrally as the fish grows to its full size[25,26].

The interaction network underlying stripe formation is being uncovered: attractive and repulsive interactions over short and long distances between both fully differentiated and

immature pigment cells are required to form the zebrafish pigment pattern[23,24,27–29]. Global factors, such as endocrine signaling, timing of differentiation, and other signals extrinsic to pigment cells provide trophic support and contribute to pattern homeostasis[30,31]. Additionally, the signaling pathways underlying each of these cellular phenomena are gradually being assigned. For example, dense iridophores in the interstripe express *colony stimulating factor 1a*, *csf1a*, the ligand for Csf1r, which is expressed by cells in the xanthophore lineage, then promotes the differentiation of unpigmented xanthoblasts into yellow xanthophores[23,32]. Unresolved, however, is how these interactions apply to stripe reiteration and if this process represents a recapitulation of stripe formation or if additional pattern elements develop by another method. In Chapter 1, I describe my work on iridophore morphology and behavior and suggest a new model for these mechanisms during interstripe reiteration.

Elucidating the cellular mechanisms responsible for stripe formation presents a unique opportunity to theorize how modulating particular nodes or the relative strength of connections could influence the resulting pattern. While *in silico* manipulations are invaluable, the genus *Danio* offers a convenient venue to test such predictions *in vivo*. Among zebrafish and closely related species exists a stunningly diverse array of pigment patterns – dark spots in *D. tinwini*, vertical bars in *D. choprae* and *D. aesculapii*, caudal eyespots in *D. erythromicron*, and shiny spots in *D. margaritatus*. Perhaps the most well-studied of these is the close relative of the zebrafish, pearl danio (*D. albolineatus*), whose apparent lack of pattern acts as the natural null hypothesis to zebrafish stripes[33]. Pearl danio have the same pigment cell types, but instead of localizing in discrete regions, melanophores, xanthophores, and iridophores are intermingled to form a uniform pattern across the flank[34]. Because of the foundational work in zebrafish, we can query specific interactions and whether they have been modified over evolutionary time. In Chapter 2, I discuss my contributions to two such studies in which we examine 1) the role of thyroid hormone as a global regulator of pigment pattern evolution and 2) the evolution of

specialized cellular projections emanating from xanthoblasts that are required for melanophore clearance and stripe consolidation[29,31].

References

1. Nüsslein-Volhard, C. & Wieschaus, E. Mutations affecting segment number and polarity in Drosophila. *Nature* **287,** 795–801 (1980).
2. Dahmann, C., Oates, A. C. & Brand, M. Boundary formation and maintenance in tissue development. *Nat. Rev. Genet.* **12,** 43–55 (2011).
3. Zecca, M., Basler, K. & Struhl, G. Sequential organizing activities of engrailed, hedgehog and decapentaplegic in the Drosophila wing. *Development* **121,** 2265–78 (1995).
4. Nellen, D., Burke, R., Struhl, G. & Basler, K. Direct and long-range action of a DPP morphogen gradient. *Cell* **85,** 357–68 (1996).
5. Irvine, K. D. & Rauskolb, C. Boundaries in development: formation and function. *Annu. Rev. Cell Dev. Biol.* **17,** 189–214 (2001).
6. Wolpert, L. Positional information and the spatial pattern of cellular differentiation. *J. Theor. Biol.* **25,** 1–47 (1969).
7. Steinberg, M. S. Differential adhesion in morphogenesis: a modern view. *Curr. Opin. Genet. Dev.* **17,** 281–286 (2007).
8. Torii, K. U. Two-dimensional spatial patterning in developmental systems. *Trends Cell Biol.* **22,** 438–46 (2012).
9. Weigelt, B., Peterse, J. L. & van 't Veer, L. J. Breast cancer metastasis: markers and models. *Nat. Rev. Cancer* **5,** 591–602 (2005).
10. Powell, D. R., Blasky, A. J., Britt, S. G. & Artinger, K. B. Riding the crest of the wave: parallels between the neural crest and cancer in epithelial-to-mesenchymal transition and migration. *Wiley Interdiscip. Rev. Syst. Biol. Med.* **5,** 511–22 (2013).
11. Millar, S. E., Miller, M. W., Stevens, M. E. & Barsh, G. S. Expression and transgenic studies of the mouse agouti gene provide insight into the mechanisms by which mammalian coat color patterns are generated. **3232,** 3223–3232 (1995).
12. Mills, M. G. & Patterson, L. B. Not just black and white: Pigment pattern development and evolution in vertebrates. *Semin. Cell Dev. Biol.* **20,** 72–81 (2009).
13. Domyan, E. T. & Shapiro, M. D. Pigeonetics takes flight: Evolution, development, and genetics of intraspecific variation. *Dev. Biol.* (2016). doi:10.1016/j.ydbio.2016.11.008
14. Gans, C. & Northcutt, R. G. Neural crest and the origin of vertebrates: a new head. *Science* **220,** 268–273 (1983).
15. Bronner, M. E. & LeDouarin, N. M. Development and evolution of the neural crest: An overview. *Dev. Biol.* **366,** 2–9 (2012).
16. Wayne, R. K. Cranial Morphology of Domestic and Wild Canids : The Influence of Development on Morphological Change Published by : Society for the Study of Evolution Stable URL : http://www.jstor.org/stable/2408805 Accessed : 22-03-2016 01 : 40 UTC Your use of the JSTO. *Evolution (N. Y).* **40,** 243–261 (1986).
17. Ziermann, J. M., Diogo, R. & Noden, D. M. Neural crest and the patterning of vertebrate craniofacial muscles. *Genesis* e23097 (2018). doi:10.1002/dvg.23097
18. Kerns, J. A. *et al.* Linkage and segregation analysis of black and brindle coat color in domestic dogs. *Genetics* **176,** 1679–1689 (2007).
19. Rawles, M. The production of robin pigment in White Leghorn feathers by grafts of embryonic robin tissue. *J. Genet.* (1939).
20. Slominski, A. *et al.* Hair follicle pigmentation. *J. Invest. Dermatol.* **124,** 13–21 (2005).
21. Yamaguchi, Y., Brenner, M. & Hearing, V. J. The regulation of skin pigmentation. *J. Biol. Chem.* **282,** 27557–27561 (2007).
22. Hirata, M., Nakamura, K. I. & Hondo, S. Pigment cell distributions in different tissues of

the zebrafish, with special reference to the striped pigment pattern. *Dev. Dyn.* **234,** 293–300 (2005).
23. Patterson, L. B. & Parichy, D. M. Interactions with Iridophores and the Tissue Environment Required for Patterning Melanophores and Xanthophores during Zebrafish Adult Pigment Stripe Formation. *PLoS Genet.* **9,** e1003561 (2013).
24. Frohnhöfer, H. G., Krauss, J., Maischein, H.-M. & Nüsslein-Volhard, C. Iridophores and their interactions with other chromatophores are required for stripe formation in zebrafish. *Development* **140,** 2997–3007 (2013).
25. Parichy, D. M., Elizondo, M. R., Mills, M. G., Gordon, T. N. & Engeszer, R. E. Normal table of postembryonic zebrafish development: staging by externally visible anatomy of the living fish. *Dev. Dyn.* **238,** 2975–3015 (2009).
26. Patterson, L. B., Bain, E. J. & Parichy, D. M. Pigment cell interactions and differential xanthophore recruitment underlying zebrafish stripe reiteration and Danio pattern evolution. *Nat. Commun.* **5,** 1–7 (2014).
27. Nakamasu, A., Takahashi, G., Kanbe, A. & Kondo, S. Interactions between zebrafish pigment cells responsible for the generation of Turing patterns. *Proc. Natl. Acad. Sci.* **106,** 8429–8434 (2009).
28. Singh, A. P. & Nusslein-Volhard, C. Zebrafish Stripes as a Model for Vertebrate Colour Pattern Formation. **25,** 81–92 (2015).
29. Eom, D. S., Bain, E. J., Patterson, L. B., Grout, M. E. & Parichy, D. M. Long-distance communication by specialized cellular projections during pigment pattern development and evolution. **4,** (2015).
30. Lang, M. R., Patterson, L. B., Gordon, T. N., Johnson, S. L. & Parichy, D. M. Basonuclin-2 requirements for zebrafish adult pigment pattern development and female fertility. *PLoS Genet.* **5,** e1000744 (2009).
31. Mcmenamin, S. K. *et al.* Thyroid hormone-dependent adult pigment cell lineage and pattern in zebrafish. *Science* **130,** 1358–1362 (2014).
32. Parichy, D. M. & Turner, J. M. Temporal and cellular requirements for Fms signaling during zebrafish adult pigment pattern development. *Development* **130,** 817–833 (2003).
33. McCluskey, B. M. & Postlethwait, J. H. Phylogeny of zebrafish, a 'model species,' within Danio, a 'model genus'. *Mol. Biol. Evol.* **32,** 635–652 (2015).
34. Quigley, I. K. *et al.* Evolutionary diversification of pigment pattern in Danio fishes: differential fms dependence and stripe loss in D. albolineatus. *Development* **132,** 89–104 (2005).

Chapter 1: Iridophore behavior and morphogenesis during interstripe reiteration

Introduction

Vertebrates have evolved a spectacular array of pigment patterns that have marked roles in ecology and animal behavior. These patterns are critical in mate choice, kin recognition, predator prey interactions, thermoregulation, and shoaling behavior along with other population dynamics[1–6]. Much of this diversity stems from the neural crest, a transient embryonic cell population that gives rise to varied cell types such as craniofacial bones and cartilage, peripheral nerves and glia, and pigment cells[7,8]. The cellular mechanisms involved in pigment pattern formation have often been studied in birds and mammals which contain a single pigment cell type, the black melanocyte. These cells synthesize pigment and then transfer it to secondary cell types such as the keratinocytes in skin and hair follicles or feathers. Melanocytes can produce two different types of melanin, the darker brownish black eumelanin and yellow reddish pheomelanin both of which contribute to the range of coloration seen in furry mammals and human skin and hair[9–11]. Conversely, ectotherms like fish, amphibians, and reptiles utilize multiple pigment cell types, called chromatophores, that retain the pigment they produce[12–14]. This makes them especially useful when studying the cellular interactions underlying pigment pattern formation as the cell types of interest contain a natural marker.

Chromatophores can also contribute to structural coloration like reflectance and iridescence. Instead of pigment containing organelles, iridescence results from the physical phenomenon of constructive interference of selected wavelengths of reflected light bouncing off subcellular structures in the dermis[15]. In the 17th century, Robert Hooke described the “gaudy” and “changeable” nature of peacock feathers lamenting that his descriptions, though tedious, were woefully insufficient as the colors shifted with even minute changes in perspective and light source[16]. With the advent of electron microscopy in the 20th century, the regularly stacked

aragonite platelets of an abalone shell[17], or the quasi-ordered collagen clusters in blue baboon scrotums[18] have been made visible and primed for new advances in the biology and structural chemistry of pigmentation.

Zebrafish is an excellent model system in which to study pigment pattern formation as it exploits several chromatophores in a highly stereotyped pattern. The adult displays three to five dark stripes made of black melanophores containing melanin, separated by lighter interstripes of pteridine and carotenoid pigments within yellow xanthophores (Figure 1A). Spread across the flank are two conformations of iridescent iridophores: dense iridophores exist in an epithelial like sheet underneath the xanthophores in each interstripe while loose iridophores are found superficial to melanophores in the stripe region and are more spread out with a dendritic appearance[19–21] (Figure 1B). Studies using this system have modeled many of the cellular interactions and environmental cues responsible for stripe formation. The dense iridophores of the primary interstripe are the first adult pigment cell type to develop, followed by melanophores differentiating on either side and coalescing into stripes and, finally, xanthophores appearing on top of the dense iridophores[19,20,22–26]. As the fish grows, new stripes and interstripes are subsequently added both dorsally and ventrally to reiterate the initial stripe pattern[27]. While stripe initiation and formation have been well studied, the process of interstripe reiteration has been largely unexplored.

Daily brightfield imaging of secondary interstripe formation (i.e., interstripe reiteration) suggests that dense iridophores delaminate from the primary interstripe, migrate through the developing stripe, and reaggregate ventrally to terminate the melanophore stripe and form the secondary interstripe[27]. This behavior is reminiscent of an EMT, or epithelial to mesenchymal transition, in which epithelial cells lose adhesive contacts with their neighbors and adopt mesenchymal qualities, including differences in shape and enhanced migration. EMT is required for migration of early neural crest in vertebrates and is also an integral step in tumor metastasis in which cancer cells break off the primary tumor, enter the bloodstream, and colonize a second

location[28–31]. In this study, we use time lapse analyses, cell tracking, and genetic manipulations to distinguish between two hypotheses for interstripe reiteration: 1) that dense iridophores in the primary interstripe undergo EMT and directly contribute to loose iridophores in the stripe and the dense secondary interstripe, and 2) iridophore cell shape is fixed so that dense and loose iridophores differentiate in their respective final locations and migrate only locally rather than long distances during interstripe reiteration (Figure 2). Our results support the latter model: dense iridophores in the interstripe remain there and new iridophores differentiate de novo in the stripe and secondary interstripe regions. We then test whether a cell shape change between loose and dense could potentially occur by challenging iridophores en masse. We find that iridophore shape is not plastic, a dense iridophore remains dense and loose remains loose, and we discuss possible cellular structures that prevent such a transition. Together, these results advance our understanding of a rapidly growing model of zebrafish pigment pattern formation and offer an alternative to previous interpretations of iridophore morphogenesis[21,32,33].

Results

Iridophores exhibit dynamic behavior during interstripe reiteration

To test whether dense iridophores from the interstripe region directly contribute to other pattern elements, we used time lapse analyses to examine iridophore behavior during four different stages of interstripe reiteration (Figure S1). We followed iridophores using a membrane targeted fluorophore (*Tg*(*pnp4a:membrane-mCherry*) with robust expression in both dense and loose conformation (Figure 3). At early stages, we found several examples of loose iridophores differentiating among melanophores (Figure 3A) in the developing stripe and loose iridophores migrating from their initial location (Figure 3B). By far the most common behavior was

proliferation (Figure 3C). During these early stages, up to 30% of loose iridophores divided over a 15-hour time lapse. Interestingly, dense iridophores in the interstripe also proliferated but much less frequently than their loose counterparts. Proliferation dropped precipitously as loose iridophores filled the stripe region and dense iridophores formed the ventral secondary interstripe (Figure 3D). We observed no examples of dense iridophores delaminating from the primary interstripe to migrate through the developing stripe in over 300 hours of time lapse imaging.

Iridophores from the primary interstripe do not contribute to the rest of the interstripe pattern

Given the necessarily limited duration of time lapse imaging, it is formally possible that we missed dense iridophores undergoing an EMT-like event. To further test this possibility, we sought to track a population of dense iridophores throughout interstripe development. We generated a double transgenic line in which iridophores were marked with both a membrane targeted fluorophore and their nuclei with photoconvertible protein EosFP (Eos) [*Tg*(*pnp4a:membrane-mCherry; pnp4a:nuclear-Eos*]. In its native form, Eos emits a strong green fluorescence (516 nm) that permanently changes to red (581 nm) upon near-UV irradiation[34]. Eos is a valuable tool for tracking cells as the photoconversion from green to red is permanent, especially when nuclear localized, and the red form perdures even after it is transferred to daughter cells[25,35]. Prior to photoconversion, iridophores have red membranes with green nuclei, but after short exposure to a 405 nm laser, the membranes remain red and the green Eos has been fully converted to red as well. Photoconversion only occurs for protein already present, yet *pnp4a* is constitutively active so newly synthesized protein is green. The combination of both the green and red form i.e. photoconverted and non-photoconverted

protein, results in photoconverted cells having white nuclei as these channels are imaged separately (Figure 4A).

To track dense iridophores through interstripe reiteration, we photoconverted a large portion of the burgeoning interstripe before reiteration occurs. If these cells contribute to the loose iridophores in the stripe, or dense iridophores in the secondary interstripe, then we would expect to see white nuclei in these regions upon completion of interstripe reiteration. Instead, we found that photoconverted dense iridophores remained in their original location in the primary interstripe (Figure 4B). Loose iridophores in the stripe and dense iridophores in the secondary interstripe exhibited green nuclei, without red fluorescence, indicating they were newly differentiated since the photoconversion and not derived from the primary interstripe (Figure 4B').

Iridophores conformation is fixed

It has become increasingly clear that iridophores play a pivotal role in pattern formation. A tenet of this model, however, suggests that patterning occurs in a two-dimensional sheet of iridophores switching between two distinct morphological states: loose and dense[23,32]. While we have not found evidence of this transition during ontogeny, we sought to test the plasticity of iridophore conformation by challenging iridophores en masse. To do this, we took advantage of the tight correlation between loose iridophores and melanophores to the exclusion of dense iridophores (Figure 1B). This correlation is maintained even in instances of aberrant patterns in zebrafish in which mutations that autonomously affect melanophore function disrupt stripe patterning (Figure S2). We used a temperature sensitive allele of *melanocyte inducing transcription factor a (mitfa*^{vc7})[36,37] to alter melanophore abundance in fish with complete adult pigment patterns. During normal development, *mitfa* acts within melanophores to promote their survival and differentiation. These mutants when raised at the permissive temperature (22°C)

are indistinguishable from wild-type, exhibiting a wild-type complement of melanophore stripes and iridophore interstripes. When reared at restrictive temperatures, however, *mitfa*^{vc7} mutants fail to form stripes and have an expanded dense iridophore interstripe.

Using a similar photoconversion paradigm as experiments above, we photoconverted all dense iridophores in *mitfa*^{vc7} mutants raised at the restrictive temperature and then shifted them to the permissive temperature. Over several days, melanophores differentiated first broadly along the flank and then coalesced into stripes similar to those of wild-type. We found that instead of dense iridophores becoming loose in association with the developing melanophores, new loose iridophores differentiated on top of new melanophores and the photoconverted dense iridophores remained in the melanophore free regions (Figure 5A). In the reciprocal experiment, mutants were raised at permissive temperature and shifted to restrictive temperature, in which melanophores died. Interestingly, this experiment illustrates a previously undescribed requirement for *mitfa* during melanophore homeostasis and pattern maintenance. New dense iridophores differentiated in the space previously occupied by melanophores suggesting loose iridophores are not able to change their conformation (Figure 5B).

Discussion

Zebrafish offer an unparalleled system in which to study the cellular behaviors underlying pattern formation in post-embryonic tissues. Interactions between the black melanophores and yellow xanthophores have been the most widely studied and the iridophores, if mentioned at all, have been treated as single population of cells. Here, we argue that dense and loose represent distinct classes of iridophore shape that are not interchangeable and have different morphogenic properties. During interstripe reiteration, loose iridophores are highly dynamic displaying rapid proliferation to fill in the melanophore stripe region. Interestingly,

expansion of the dense primary interstripe also relies on proliferation, but at a slower rate. Cell tracking over the course of several weeks suggests dense iridophores do not delaminate from the primary interstripe as we, and others, have speculated in the past[21,32,33,38].

Recently, we have examined potential cellular reasons underlying the fixed nature of iridophore morphology. Iridophores derive their iridescence from reflective guanine platelets contained within membrane-bound organelles[17,39]. When illuminated with reflected light dense iridophores appear gold and loose iridophores appear blue. This suggests that the arrangement of the platelets inside the two different conformations of iridophores could be different. If this hypothesis is correct, then any shape changes between dense and loose would require the iridophore to dissolve its reflecting platelets and reassemble them in the appropriate conformation. One could speculate this would be so metabolically expensive that, instead, iridophores die and new iridophores differentiate in the appropriate conformation. Detailed structural biochemistry analyses are required to determine the differences in platelet arrangement inside dense and loose iridophores.

Our data contribute to the growing network of pigment cell morphogenesis required to build zebrafish stripes. A particular strength of the zebrafish model is the wealth of diverse pigment patterns in closely related species in the *Danio* genus. These other species use the same pigment cell toolkit to form vertical bars, spots, spirals, and more. We can use what we have learned from zebrafish to form testable hypotheses in evolutionarily derived patterns. Given the dynamic behaviors of iridophores during stripe formation, we look forward to expanding our studies into their role in other pattern paradigms.

Materials and Methods

Fish stocks and rearing conditions, transgenesis and transgenic line production

Fish were reared under standard conditions (14L:10D at ~28˚C) and staging followed[40]. Stocks were wild-type stock fish WT(WA), or its derivative WT(ABb)[26], *mitfa*^{vc7} temperature sensitive mutants[37], *Tg*(*pnp4a-membranemCherry*)*, or Tg*(*pnp4a-palmmCherry;nlsEosFP*).

Transgenes were assembled by Gateway cloning of entry plasmids into pDest vectors containing Tol2 repeats for efficient genomic integration[41].

For cell tracking using EosFP, iridophore nuclei were converted individually or in small groups using the photobleaching tool and 405nm laser in Zeiss ZEN blue. Individuals were then reared separately in cups in heatshock tanks at 22°C (permissive) or 34°C (restrictive). Cups were covered or reared in black painted tanks to minimize light pollution and spontaneous photoconversion.

Imaging and cell counts

For imaging, fish were generally treated with epinephrine to contract pigment granules towards cell centers. Images were acquired on: Zeiss AxioObserver inverted microscopes equipped either with Axiocam HR or Axiocam 506 color cameras or a Yokogawa laser spinning disk with Evolve camera, AxioZoom v16 stereomicroscope with Axiocam 506 color camera, and LSM880 scanning laser confocal microscope with Airyscan detector all running ZEN blue or black software. Ex vivo imaging of pigment cells in their native tissue environment followed[26], with images acquired at 5-min intervals for 15 hr at 10x using an Evolve (Photometrics, Tucson, AZ) camera mounted on a Zeiss Observer Z1 inverted microscope with CSU- X1 spinning disk (Yokogawa, Tokyo, Japan). Bright-field images were taken before and after imaging. Larvae were 7.5 SSL except where indicated. All iridophores initially within regions of interest were

counted. Proliferating iridophores were evident as single cells that rounded-up and then divided to generate adjacent daughter cells.

Figure Legends

Figure 1

Iridophore morphology in adult zebrafish

(A) Stripe and interstripe pattern of adult zebrafish **(B)** Iridophore morphology in primary stripes and interstripe and secondary interstripe using transmitted light, left; reflected light, middle; and *Tg*(*pnp4a:membrane-mCherry*) to mark iridophore membranes, right. Solid lines on far left indicate stripe regions, dashed to interstripes. Colored shapes representing pigment cell classes and their relative location on either side of (B). Scale bar: 1mm, (A).

Figure 2

Two models for iridophore behavior during interstripe reiteration

The “direct contribution” model suggests dense iridophores (circles) delaminate from the primary interstripe and contribute to loose iridophores (triangles) in the stripe and reaggregate to form the dense secondary interstripe. Stars denote migratory cells in the interstripe that change shape. The “de novo differentiation” model acts as the null hypothesis in which starred dense iridophores remain in their original location and new loose and dense iridophore differentiate de novo in their final relative location. Developmental time progresses left to right.

Figure 3

Iridophores display dynamic behavior during interstripe reiteration

(A) New loose iridophore differentiates over the course of a 15-hour time-lapse (arrow). Minutes elapsed indicated in lower right for (A), (B), and (C). **(B)** Loose iridophore migrates several cell lengths away from its original location. Reference cell, dashed circle; migrating cell, arrow. **(C)** Loose iridophore rounds up and divides into two daughter cells (arrowheads). **(D)** Frequency of proliferation seen in dense and loose iridophores over the course of interstripe reiteration.

Frequency calculated by counting number of cytokinesis events over the total cells of that type in the movie. Total cells counted: 6.5mm, 2258 dense, 44 loose; 7.5mm, 5987 dense, 878 loose; 10mm, 2229 dense, 967 loose; 12mm, 1727 dense, 1170 loose.

Figure 4

Iridophores from the primary interstripe do not contribute to loose iridophores in the stripe or dense iridophores in the secondary interstripe

(A) Experimental design for photoconversion and cell tracking experiments. Iridophore membranes marked with *Tg*(*pnp4a:membrane-mCherry*) and nuclei marked with *Tg*(*pnp4a-nlsEosFP*). **(B)** Images taken immediately post photoconversion, 0 days post conversion (dpc). red channel, all membrane and photoconverted nuclei; green, all EosFP photoconverted; merge. 11dpc, interstripe reiteration is complete; red channel, all membranes and photoconverted EosFP inside nuclei; green, newly produced EosFP; merge, white nuclei were present for initial photoconversion. **(B')** Close-up images of regions of interest of 11dpc merged image. Red square, primary interstripe; yellow square, stripe; blue square, secondary interstripe.

Figure 5

Iridophore conformation is fixed

(A) *mitfa*^{vc7} *Tg*(*pnp4:membrane-mCherry*); mosaic (*pnp4a:nuclearEosFP*) raised at the permissive temperature, 22°C, blue bar, and switched to restrictive temperature, 33°C (melanophores die, red bar). Solid lines indicate dense iridophores, dashed lines are loose iridophores at experiment starting point. Similar photoconversion paradigm as Figure 4; after 47 days at the restrictive temperature, white nuclei indicate iridophores that were present for the initial photoconversion, green nuclei are newly differentiated. Inset shows newly differentiated iridophores in the area previously occupied by melanophores **(B)** *mitfa*^{vc7} *Tg*(*pnp4:membrane-*

mCherry); mosaic (*pnp4a:nuclearEosFP*) raised at restrictive temperature (no melanophores differentiate, red bar) and shifted to the permissive temperature (blue bar). Insets show the relative density of dense iridophores at the beginning and end of the experiment.

Figure S1

Stages examined during time lapse analyses

Representative images of iridophores during time-lapse analyses: 6.5 SL, 7.5 SL, 10 SL, and 12 SL. Brightfield images modified from[40].

Figure S2

Zebrafish mutants with aberrant stripe patterns maintain separation of melanophores and dense iridophores

Adult pigment pattern detail, gene indicated in lower right where applicable; *bonparte* (*bnc2*)[42], *picasso* (*erbb3b*^{wpr22e2})[43], *pissaro*, *puma* (*tuba8l3a*)[44], *seurat* (*igsf11*)[45], *leopard* (*cx41.8*)[46].

References

1. Endler, J. A. Natural Selection on Color Patterns in Poecilia reticulata Author (s): John A . Endler Published by : Society for the Study of Evolution Stable URL : http://www.jstor.org/stable/2408316 REFERENCES Linked references are available on JSTOR for this articl. **34,** 76–91 (2016).
2. Engeszer, R. E., Wang, G., Ryan, M. J. & Parichy, D. M. Sex-specific perceptual spaces for a vertebrate basal social aggregative behavior. *Proc. Natl. Acad. Sci. U. S. A.* **105,** 929–33 (2008).
3. Mills, M. G. & Patterson, L. B. Not just black and white: Pigment pattern development and evolution in vertebrates. *Semin. Cell Dev. Biol.* **20,** 72–81 (2009).
4. Price, A. C., Weadick, C. J., Shim, J., Rodd, F. H. & Al, P. E. T. Pigments , Patterns , and Fish Behavior. **5,** (2008).
5. Houde, A. *Sex, Color, and Mate Choice in Guppies*. (Princeton University Press, 1997).
6. Finkbeiner, S. D., Briscoe, A. D. & Reed, R. D. Warning signals are seductive: Relative contributions of color and pattern to predator avoidance and mate attraction in Heliconius butterflies. *Evolution* 1–35 (2014). doi:10.1111/evo.12524
7. Le Douarin, N. & Kalcheim, C. *The Neural Crest*. (Cambridge University Press, 1999).
8. Gans, C. & Northcutt, R. G. Neural crest and the origin of vertebrates: a new head. *Science* **220,** 268–273 (1983).
9. Barsh, G. Regulation of pigment type switching by Agouti, melanocortin signaling, Attractin and Mahoganoid. in *The pigmentary system: physiology and pathophysiology* (eds. Nordlund, J. et al.) 395 (Blackwell Publishing, 2006).
10. Slominski, A. *et al.* Hair follicle pigmentation. *J. Invest. Dermatol.* **124,** 13–21 (2005).
11. Yamaguchi, Y., Brenner, M. & Hearing, V. J. The regulation of skin pigmentation. *J. Biol. Chem.* **282,** 27557–27561 (2007).
12. Parichy, D., Reedy, M. & Erickson, C. Regulation of melanoblast migration and differentiation. in *The pigmentary system: physiology and pathophysiology* (eds. Nordlund, J. et al.) (Blackwell Publishing, 2006).
13. Fujii, R. The regulation of motile activity in fish chromatophores. *Pigment Cell Res.* **13,** 300–319 (2000).
14. Kelsh, R. N. Genetics and evolution of pigment patterns in fish. *Pigment Cell Research* **17,** 326–336 (2004).
15. Gur, D., Leshem, B., Oron, D., Weiner, S. & Addadi, L. The structural basis for enhanced silver reflectance in Koi fish scale and skin. *J. Am. Chem. Soc.* **136,** 17236–17242 (2014).
16. Hooke, R. *Micrographia*. (The Royal Society, 1665).
17. Tan, T., Wong, D. & Lee, P. Iridescence of a shell of mollusk Haliotis glabra. *Opt. Express* **12,** 4847–4854 (2004).
18. Prum, R. O. Structural colouration of mammalian skin: convergent evolution of coherently scattering dermal collagen arrays. *J. Exp. Biol.* **207,** 2157–2172 (2004).
19. Frohnhofer, H. G., Krauss, J., Maischein, H.-M. & Nusslein-Volhard, C. Iridophores and their interactions with other chromatophores are required for stripe formation in zebrafish. *Development* **140,** 2997–3007 (2013).
20. Patterson, L. B. & Parichy, D. M. Interactions with Iridophores and the Tissue Environment Required for Patterning Melanophores and Xanthophores during Zebrafish Adult Pigment Stripe Formation. *PLoS Genet.* **9,** e1003561 (2013).
21. Singh, A. P., Schach, U. & Nüsslein-Volhard, C. Proliferation, dispersal and patterned aggregation of iridophores in the skin prefigure striped colouration of zebrafish. *Nat. Cell Biol.* **16,** 607–14 (2014).
22. Nakamasu, A., Takahashi, G., Kanbe, A. & Kondo, S. Interactions between zebrafish pigment cells responsible for the generation of Turing patterns. *Proc. Natl. Acad. Sci.*

106, 8429–8434 (2009).
23. Singh, A. P. & Nusslein-Volhard, C. Zebrafish Stripes as a Model for Vertebrate Colour Pattern Formation. **25,** 81–92 (2015).
24. Patterson, L. B. & Parichy, D. M. Melanophores Tune Out the Noise to Make Stripes. *Dev. Cell* 544–545 (2018). doi:10.1016/j.devcel.2018.05.014
25. Mcmenamin, S. K. *et al.* Thyroid hormone-dependent adult pigment cell lineage and pattern in zebrafish. *Science* **130,** 1358–1362 (2014).
26. Eom, D. S., Bain, E. J., Patterson, L. B., Grout, M. E. & Parichy, D. M. Long-distance communication by specialized cellular projections during pigment pattern development and evolution. **4,** (2015).
27. Patterson, L. B., Bain, E. J. & Parichy, D. M. Pigment cell interactions and differential xanthophore recruitment underlying zebrafish stripe reiteration and Danio pattern evolution. *Nat. Commun.* **5,** 1–7 (2014).
28. Diepenbruck, M. & Christofori, G. Epithelial–mesenchymal transition (EMT) and metastasis: yes, no, maybe? *Curr. Opin. Cell Biol.* **43,** 7–13 (2016).
29. Theveneau, E. & Mayor, R. Neural crest delamination and migration: From epithelium-to-mesenchyme transition to collective cell migration. *Dev. Biol.* **366,** 34–54 (2012).
30. Bronner, M. E. & LeDouarin, N. M. Development and evolution of the neural crest: An overview. *Dev. Biol.* **366,** 2–9 (2012).
31. Steinberg, M. S. Differential adhesion in morphogenesis: a modern view. *Curr. Opin. Genet. Dev.* **17,** 281–286 (2007).
32. Volkening, A. & Sandstede, B. Iridophores as a source of robustness in zebrafish stripes and variability in Danio patterns. *Nat. Commun.* **9,** 1–14 (2018).
33. Fadeev, A., Krauss, J., Frohnhöfer, H. G., Irion, U. & Nüsslein-volhard, C. Tight junction protein 1a regulates pigment cell organisation during zebrafish colour patterning. (2015).
34. Wiedenmann, J. *et al.* EosFP, a fluorescent marker protein with UV-inducible green-to-red fluorescence conversion. *Proc. Natl. Acad. Sci.* **101,** 15905–15910 (2004).
35. Nienhaus, G. U. *et al.* Photoconvertible Fluorescent Protein EosFP: Biophysical Properties and Cell Biology Applications. *Photochem. Photobiol.* **82,** 351 (2006).
36. Lister, J. A., Robertson, C. P., Lepage, T., Johnson, S. L. & Raible, D. W. nacre encodes a zebrafish microphthalmia-related protein that regulates neural-crest-derived pigment cell fate. *Development* **3767,** 3757–3767 (1999).
37. Johnson, S. L., Nguyen, A. N. & Lister, J. a. Mitfa Is Required At Multiple Stages of Melanocyte Differentiation But Not To Establish the Melanocyte Stem Cell. *Dev. Biol.* **350,** 405–13 (2011).
38. Walderich, B., Singh, A. P., Mahalwar, P. & Nüsslein-Volhard, C. Homotypic cell competition regulates proliferation and tiling of zebrafish pigment cells during colour pattern formation. *Nat. Commun.* **7,** 11462 (2016).
39. Hirata, M., Nakamura, K. I. & Hondo, S. Pigment cell distributions in different tissues of the zebrafish, with special reference to the striped pigment pattern. *Dev. Dyn.* **234,** 293–300 (2005).
40. Parichy, D. M., Elizondo, M. R., Mills, M. G., Gordon, T. N. & Engeszer, R. E. Normal table of postembryonic zebrafish development: staging by externally visible anatomy of the living fish. *Dev. Dyn.* **238,** 2975–3015 (2009).
41. Kwan, K. *et al.* The Tol2kit: a multisite gateway-based construction kit for Tol2 transposon transgenesis constructs. *Dev. Dyn.* **236,** 3088–99 (2007).
42. Lang, M. R., Patterson, L. B., Gordon, T. N., Johnson, S. L. & Parichy, D. M. Basonuclin-2 requirements for zebrafish adult pigment pattern development and female fertility. *PLoS Genet.* **5,** e1000744 (2009).
43. Budi, E. H., Patterson, L. B. & Parichy, D. M. Embryonic requirements for ErbB signaling in neural crest development and adult pigment pattern formation. *Development* **135,**

2603–14 (2008).
44. Larson, T. A., Gordon, T. N., Lau, H. E. & Parichy, D. M. Defective adult oligodendrocyte and Schwann cell development, pigment pattern, and craniofacial morphology in puma mutant zebrafish having an alpha tubulin mutation. *Dev. Biol.* **346,** 296–309 (2010).
45. Eom, D. S. *et al.* Melanophore migration and survival during zebrafish adult pigment stripe development require the immunoglobulin superfamily adhesion molecule Igsf11. *PLoS Genet.* **8,** e1002899 (2012).
46. Watanabe, M. *et al.* Spot pattern of leopard Danio is caused by mutation in the zebrafish connexin41.8 gene. *EMBO Rep.* **7,** 893–7 (2006).

Figure 1

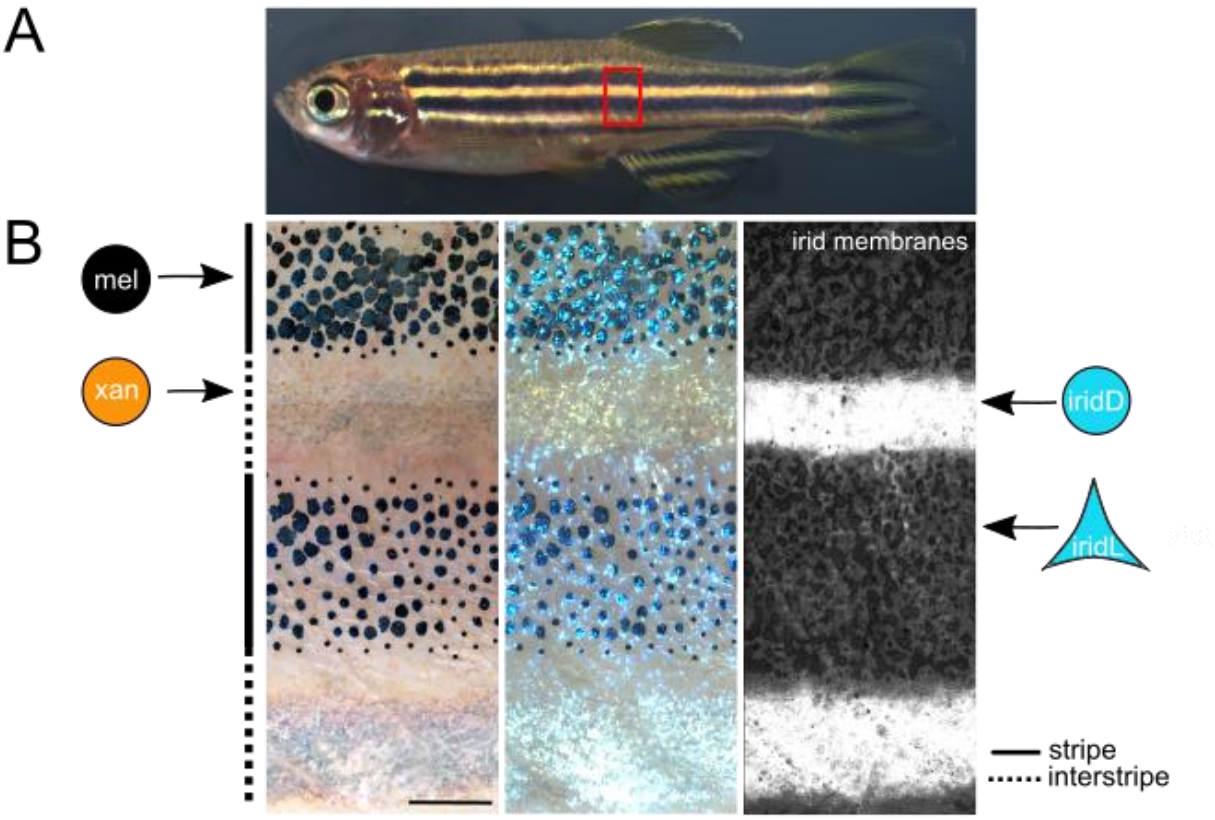

Figure 2

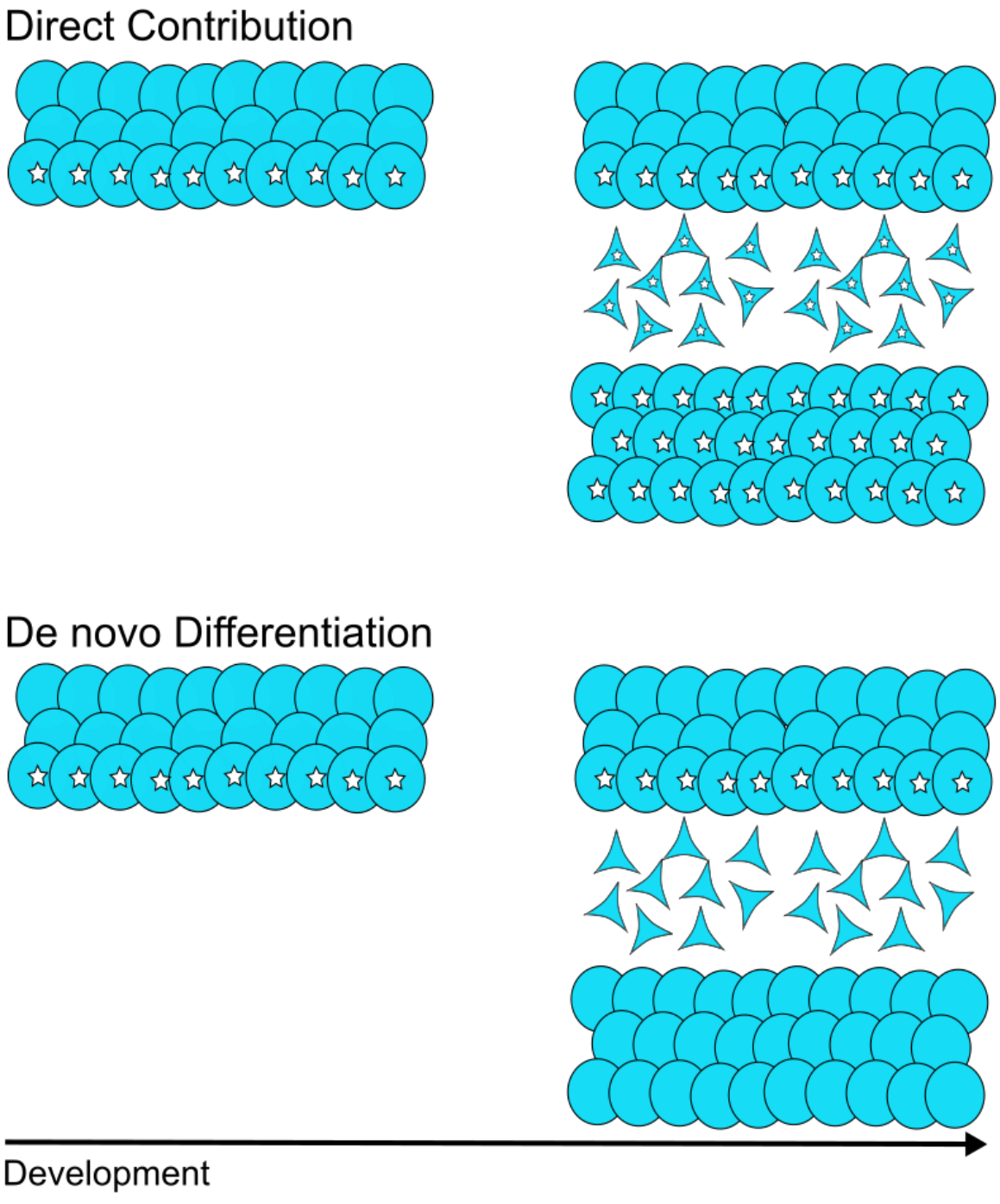
Direct Contribution
De novo Differentiation
Development

Figure 3

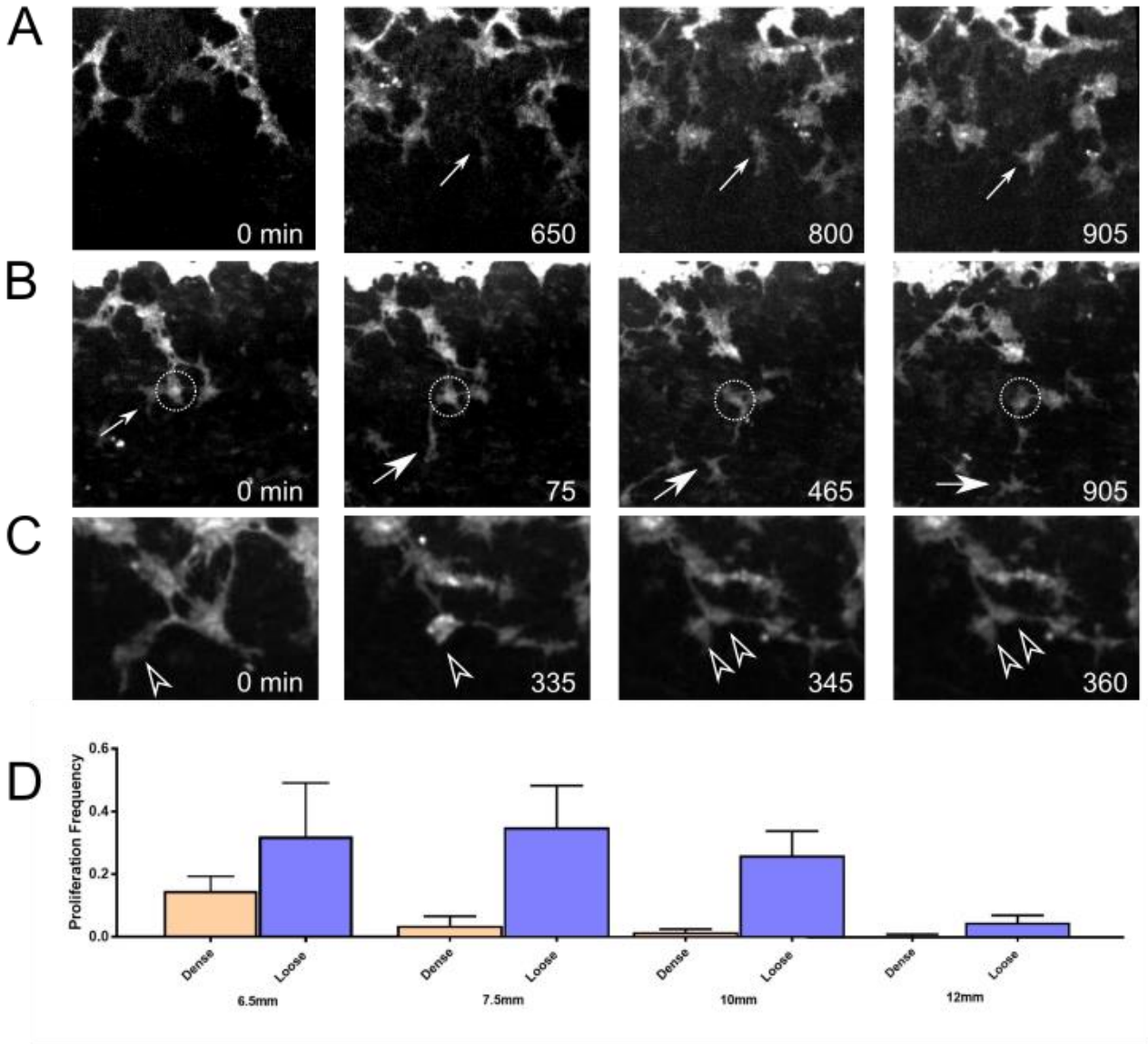
A
0 min
650
800
905
B
0 min
75
465
905
C
0 min
335
345
360
D
Proliferation Frequency
0.6
0.4
0.2
0.0
Dense
Loose
6.5mm
7.5mm
10mm
12mm

Figure 4

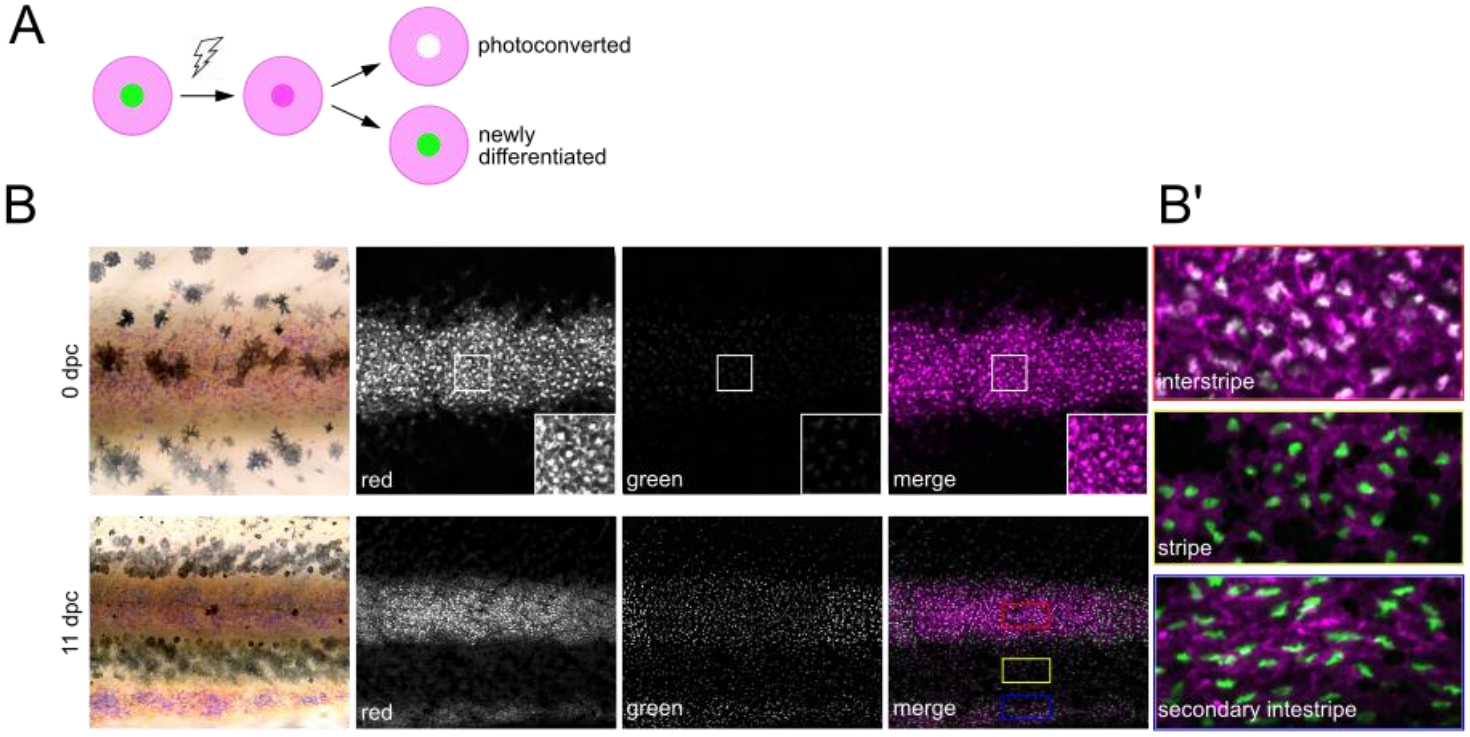
A
photoconverted
newly
differentiated
B
B'
0 dpc
11 dpc
red
green
merge
red
green
merge
interstripe
stripe
secondary intestripe

Figure 5

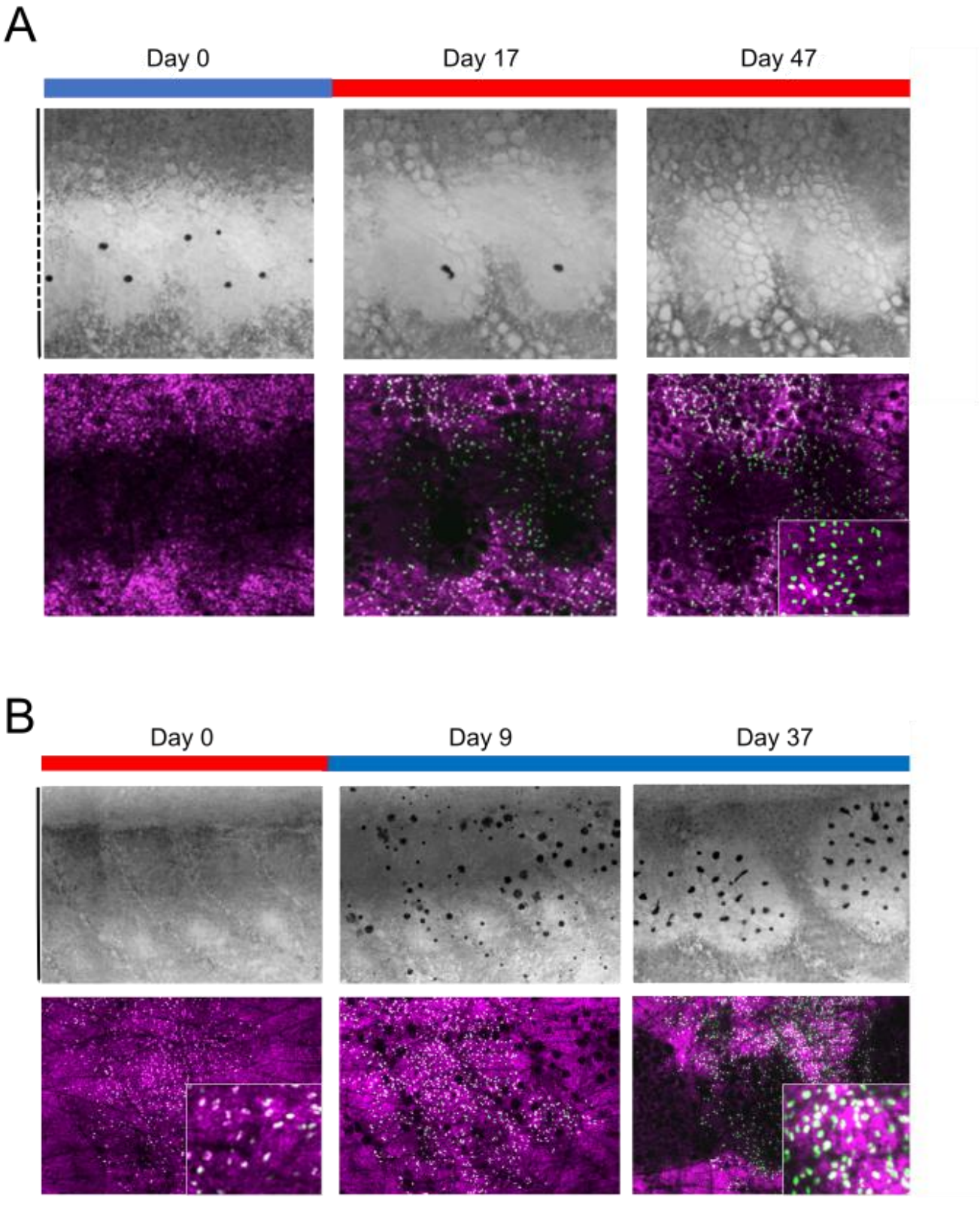

Figure S1

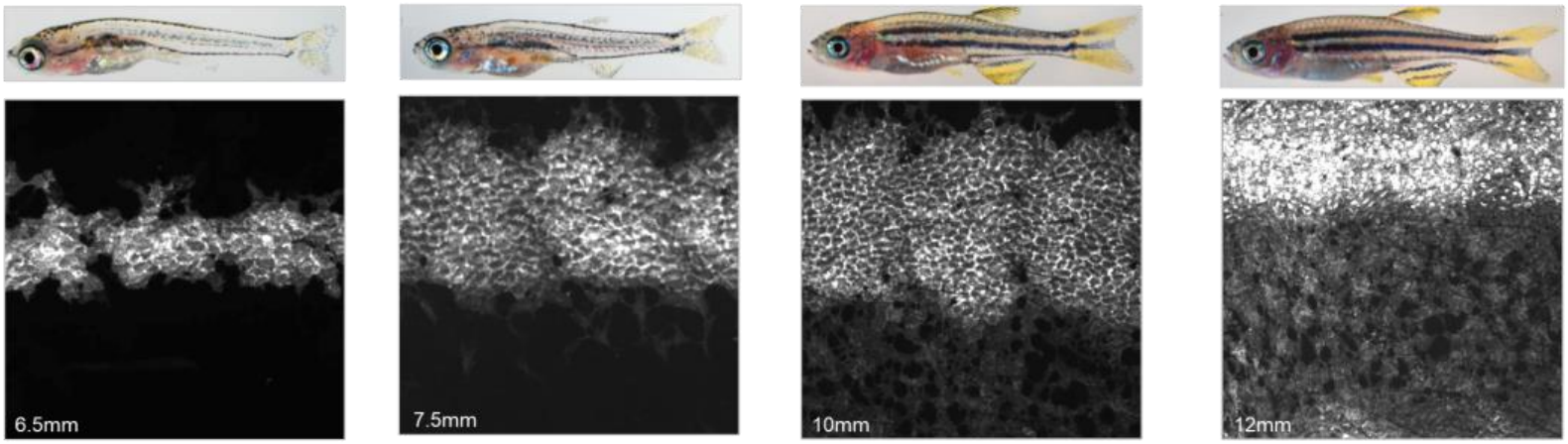

Figure S2

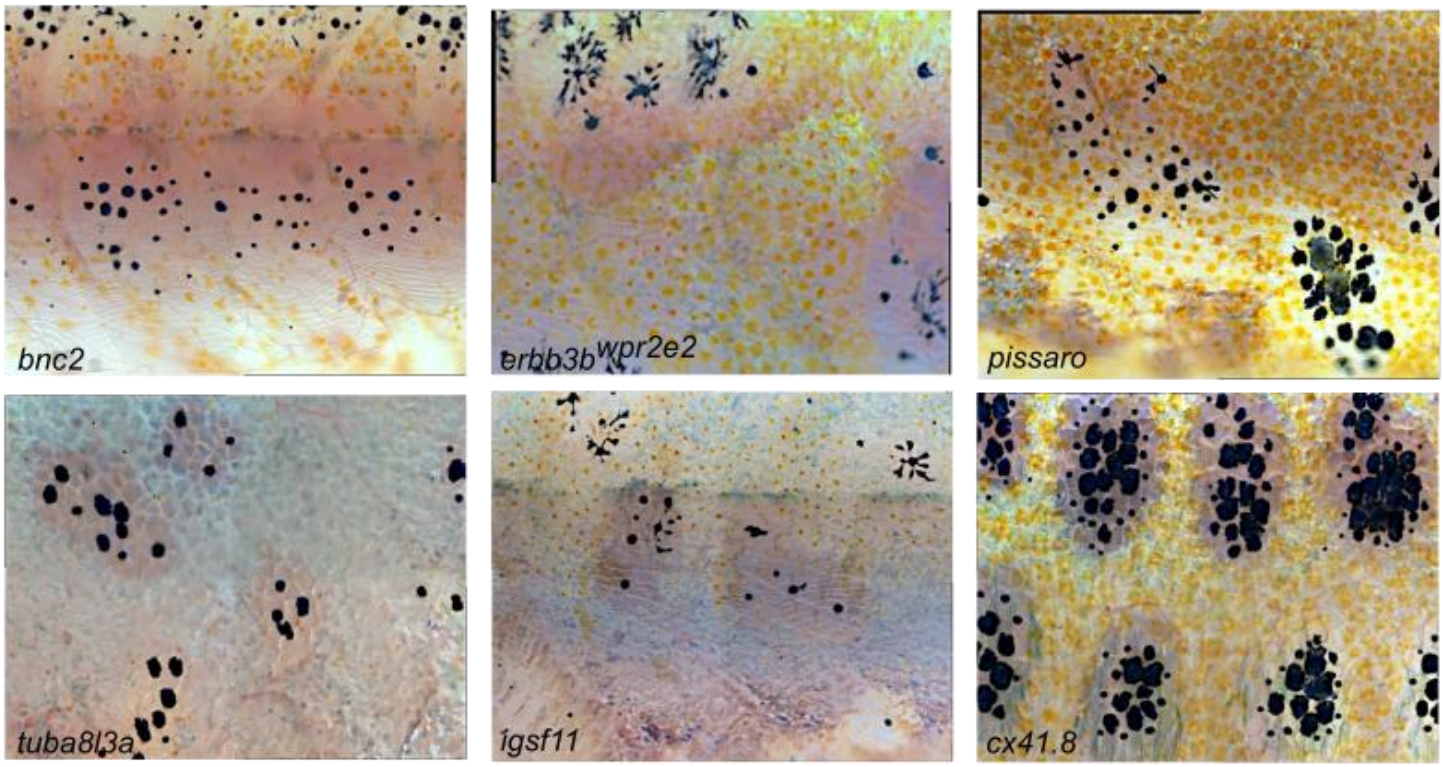

Chapter 2: Evolution of cellular interactions during pigment pattern formation

Data in this chapter published in the following articles:

McMenamin, S., Bain, E., *et al*. (2014) Thyroid hormone dependent adult pigment cell lineage and pattern in zebrafish. *Science* 345(6202): 1358-61 PMC4211621

Eom, D., Bain, E., Patterson, L., Grout, M., and Parichy, D. (2015) Long distance communication by specialized cellular projections during pigment pattern development and evolution. *eLife* 4:e12401 PMC4764569

Introduction

Vertebrates exhibit a stunning variety of pigment patterns, yet the mechanisms underlying pattern development and evolution are only beginning to be discovered. Among the most conspicuous and elaborate patterns are those of teleost fishes, which function in mate choice, shoaling, camouflage, and speciation[1–3]. The biomedical model organism zebrafish, *Danio rerio*, has a stereotyped pattern of dark stripes of black melanophores and loose iridophores separated by lighter interstripes of yellow xanthophores and densely packed iridescent iridophores (Figure 1A). To produce such a robust pattern requires interactions between the pigment cells themselves, both attractive and repulsive over short and long distances[4–8]. Additionally, environmental factors supply positional cues for the early differentiated pigment cells as well as trophic support, later localization, and maintenance of pattern boundaries[9,10] (Figure 1B). While much of this pattern formation has been described

phenomenologically at the cellular level, the molecular mechanisms underlying these processes are just beginning to be explored.

Among the strengths of zebrafish pigment pattern as a model, is the incredible diversity of patterns in other *Danio* fishes. Even those species most closely related to zebrafish display pigment patterns ranging from vertical bars in *D. aesculapii*, spots in *D. tinwini*, and spots and stripes in *D. nigrofasciatus*[11]. By generating a model for pigment pattern formation in a well-studied species like zebrafish, we can form testable hypotheses as to how these pattern variants evolve over time. To this end, we chose to study the pearl danio, *D. albolineatus*, as it is was once considered zebrafish's closest relative[12], but also because its pattern lies on the opposite end of the stripe spectrum. Pearl danio have the same pigment cells types as the zebrafish, black melanophores, yellow xanthophores, and iridescent iridophores, but instead of being organized into stripes they are intermingled across the flank offering a uniform pattern (Figure 1A).

Here, we explore two specific nodes in the pigment cell interaction diagram and ask how each has evolved between zebrafish and pearl danio. First, we show that thyroid hormone is a global regulator of pigment cell differentiation with subsequent consequences for patterning and that this role for thyroid hormone is conserved in one population of pearl danio xanthophores, but not another (Figure 1B – red square). We then show that signaling from specialized cellular processes called "airinemes" involved in stripe consolidation and melanophore clearance from the interstripe, has been evolutionarily lost in pearl danio (Figure 1B – red arrowhead). These results identify two specific cellular changes that contribute to the uniform pattern of pearl danio and highlight the adaptability of information gleaned from the zebrafish model system when studying new pattern paradigms.

Results

Thyroid hormone regulates xanthophore differentiation in pearl danio

Thyroid hormone has long been studied as a mediator of abrupt metamorphoses in amphibians and flatfishes[13–17]. To study its effect in zebrafish and closely related species we generated a transgenic line in both zebrafish and pearl danio in which the thyroid follicles express nitroreductase (Ntr) [*Tg(tg:nVenus-2a-nfnB*$^{wp.rt8}$]. Ntr converts the pro-drug Metronidazole (Mtz) into toxic metabolites that kill cells expressing the transgene[18]. When we ablated the thyroid gland at 4 days post fertilization (dpf) and followed the fish into adulthood, both zebrafish and pearl danio failed to develop most pigmented xanthophores in the hypodermis (Figure 2A). Additionally, there was an increase in melanophores along the flank in both species suggesting that thyroid hormone promotes xanthophore differentiation while inhibiting melanophore differentiation during ontogeny (Figure 2B).

Extra-hypodermal xanthophores in pearl danio develop independently of thyroid hormone signaling

We were intrigued further by the connection between thyroid hormone and xanthophore differentiation as pearl danio phenotypically resembled the zebrafish mutant *opallus*^{b1071} which harbors a missense mutation (Asp^{632} → Tyr) in *thyroid stimulating hormone receptor* (*tshr*) that causes constitutive Tshr activity. Interestingly, this mutation is identical to a human mutation underlying genetic hyperthyroidism[19]. *opallus* mutants showed a dramatic increase in the number of pigmented xanthophores on the flank, but they also had another population of 'extra-hypodermal' xanthophores that exist deep to the skin in the muscle tissue[10]. Pearl danio have a

similar population of deep xanthophores, though these were still present after thyroid ablation suggesting they are not thyroid hormone dependent (Figure 2A).

Cells of the xanthophore lineage in pearl danio do not extend airinemes as frequently as those in zebrafish

Given the importance of xanthophores in pearl danio pattern[20], we queried the interaction between unpigmented xanthoblasts in the stripe region and their role in stripe consolidation and melanophore clearance as an evolutionary target. In zebrafish, unpigmented xanthoblasts in the stripe region extend specialized projections, “airinemes,” that preferentially stabilized on either newly differentiated melanophores trespassing in the interstripe or early larval (EL) melanophores (Figure 3A). EL melanophores are remnants of the embryonic pigment pattern and only minimally contribute to the adult stripes[4,21–23]. We can visualize the cells of the xanthophore lineage by their expression of *aldehyde oxidase 5* (*aox5*; formerly, *aox3*) and a membrane targeted fluorophore in both species (Figure 3A). These projections were especially frequent during the early stages of stripe formation in zebrafish (Figure 3B). In contrast, airinemes were very rare in pearl danio across all stages of pattern formation examined (Figure 3C). When we blocked airinemes extension altogether, we saw defects in melanophore clearance in the interstripe (Figure 3D) suggesting that airinemes are required for stripe consolidation.

Blocking xanthophore terminal differentiation in pearl danio increases airinemes extension frequency

Previous work in pearl danio showed that early, widespread differentiation of xanthophores likely attenuates the positional information available to melanophores resulting in

the intermingling of melanophores and xanthophores and, consequently, production of the uniform pattern[20]. Combined with the work in zebrafish showing that airinemes extension is differentiation state dependent, we hypothesized that pearl danios exhibit fewer *aox5*+ airinemes owing to the precocious differentiation of their xanthophores. To test this, we experimentally arrested the differentiation of xanthoblasts to xanthophores by ablating the thyroid using the *tg*:NTR transgenic line already generated in pearl danio. Consistent with our hypothesis, we found an increase in the frequency of airinemes extension in *aox5*+ cells during early stages of pattern formation, but not to the extent that we see in zebrafish (Figure 4A, left).

Species difference in airineme production is non-autonomous to the xanthophore lineage

To test if species differences in airinemes production reflect evolutionary changes that are autonomous or non-autonomous to the xanthophore lineage, we transplanted cells between zebrafish and pearl danio[24,25]. Zebrafish *aox5*+ cells in pearl danio hosts extended airinemes at reduced frequencies, similar to that of pearl danio *aox5*+ cells (Figure 4A, right, Figure 4B). We interpret this observation, as well as *aox5*+ cell behaviors in reciprocal transplants, and adult pigment patterns of chimeras, as indicating species differences that are non-autonomous to the xanthophore lineage (Figure S1). These results are consistent with prior analyses that implicated *cis*-regulatory changes affecting environmentally produced xanthogenic Csf1 in the earlier and broader differentiation of xanthophores and altered melanophore pattern of pearl danio[20]. We therefore asked whether Csf1 alone could be responsible for species differences in airinemes production. Consistent with this idea, over expression of Csf1 in zebrafish resulted in a 22% reduction in airinemes frequency within 24 hours and an 86% reduction after complete xanthophore differentiation, as in pearl danio (Figure 4A, right).

Together, these results support the interpretation that infrequent airineme extension, as well as pattern differences in pearl danio as compared to zebrafish, arise at least in part from

evolutionary changes in factors extrinsic to the xanthophore lineage. Furthermore, our work identifies Csf1 as an especially good candidate for mediating these effects.

Discussion

In these analyses, we illustrate how elucidating mechanisms of pigment cell behavior in the model system zebrafish can provide a wealth of testable hypotheses to explain evolution of pattern formation between closely related species. We highlight the differences in pattern between the striped zebrafish and the uniform pattern of pearl danio in which all the pigment cell types are intermingled across the flank. Overall, pearl danio have substantially more fully differentiated xanthophores both superficial and deep than their striped counterparts as well as a decrease in black melanophores resembling a zebrafish mutant with an increase in thyroid hormone signaling. We found that pearl danio requires thyroid hormone signaling for its full complement of differentiated xanthophores along the flank; however, the deep xanthophore population remains intact upon ablation of the thyroid (Figure 5A). Additionally, thyroid hormone signaling is conserved in other aspects of morphology like craniofacial bone structure, barbel development, and fin fragility (Figure S2)[10]. These differences raise the possibility of a new compensatory factor in pearl danio that is responsible for the attenuation of the effects of thyroid hormone signaling in peal danio.

With our work on airineme signaling in the uniformly patterned pearl danio we link evolutionary genetic modifications to morphogenetic behaviors occurring during the development of a very different, naturally occurring phenotype. Interspecific transplants and transgenic manipulations together suggest a model in which enhanced Csf1 expression drives precocious, widespread xanthophore differentiation, limiting positional information available to melanophores[20], as well as airineme production and the potential for melanophore migration and stripe consolidation (Figure 5B). These findings do no exclude roles for additional factors;

e.g., melanophore-autonomous differences, or changes in iridophore patterning that may or may not themselves be xanthophore-dependent. Nevertheless, by focusing at high resolution on cellular behaviors our study has provided insights into the evolution of an alternative pattern state that could not have been anticipated from the analyses of genetic variation and gene regulatory differences alone. These findings illustrate how an iterative approach with model organisms and closely related species can provide insights into mechanisms by which evolutionary changes in gene activity are translated through morphogenetic behaviors in species differences in form.

Together, our results suggest responsiveness to “global” factors such as thyroid hormone should be considered along with modifications to “local” interactions, such as airineme extension, in attempting to understand pattern development and evolution.

Materials and Methods

Staging, rearing, and stocks

Staging followed[26] and fish were maintained at 28.5˚C, 16:8 L:D. Zebrafish were wild-type AB^{wp} or its derivative WT(ABb), hyperthyroid *opallus*^{b1071} (tshr^{D632Y}), *Tg(tg:nVenus-2a-nfnB)*$^{wp.rt8}$, *Tg(aox5:palmEGFP)*$^{wp.rt22}$ [10]*.* Pearl danio *D.*aff. *albolineatus*[27] were wild type, *Tg(tg:nVenus-2a-nfnB)*$^{wp.at3}$ [10] and *Tg(aox5:palmEGFP)*$^{wp.at4}$. All thyroid-ablated (Mtz-treated) and control (DMSO-treated) *Tg(tg:nVenus-v2a-nfnB)* fish were kept under TH-free conditions, fed only Artemia and rotifers enriched with TH-free Algamac (Aquafauna) and kept in static water tanks changed weekly.

Transgenesis and transgenic line production

Transgenesis employing Tol2 transposase, as well as Gateway Tol2kit and other vectors followed standard procedures[28,29]. To ablate TH-producing thyroid follicles, we cloned 514 bp 5' to the *tg* start site and used it to drive nuclear localized Venus linked by viral 2a sequence to Ntr, encoded by *nfnB*[18]*.* We generated stable lines using this construct in both *D. rerio* and *D. albolineatus*. To visualize *aox5* cells in non-mosaic fish we generated transgenic lines by BAC recombineering to express membrane targeted, palmitoylated GFP; we additionally subcloned ~12 kb of this BAC and used it to generate *Tg(aox3[8.0]:palmGFP)*$^{wp.rt12}$, containing 8.0 kb of native *aox5* sequence, which exhibited an expression pattern indistinguishable from that of the BAC.

Nitroreductase-mediated cell ablation

To ablate thyroid follicles of *tg:nVenus-2a-nfnB D. rerio* or *D. albolineatus*, we incubated 4 dpf larvae for 4 h in either 10 mM Mtz with 1% DMSO, or 1% DMSO alone. Thyroid ablations of

juveniles were performed on 4 month-old [J++, 15–17 mm standard length (SL)[26]] transgenic fish incubated for 24 h with Mtz or DMSO. For all thyroid ablations, treated individuals were assessed for loss of nVenus the following day; the absence of regeneration was subsequently assayed by the absence of nVenus expression. For heat shock, *Tg (hsp70:csf1a-DrIRES-nCFP)* larvae were exposed 1 hr to 38˚C twice daily between 6.5–7.0 SSL and 7.5 SSL

Repeated image series

For time-course imaging of pigment pattern development, WT and *opallus* individuals, as well as *Tg(tg:nVenus-2a-nfnB)* DMSO-treated and Mtz-treated siblings were imaged daily beginning at stages CR/DC (~5 SL) and continuing through development of an adult pattern [J++, or the stage of anterior scale appearance (SA) for thyroid-ablated fish in which scales develop very late]. Fish were reared individually in beakers, treated with epinephrine to contract pigment granules, briefly anesthetized in MS222, imaged, then allowed to recover and returned to their beakers. Images were taken of the same region, at the middle of the flank just posterior to the anus, on a Zeiss Observer inverted compound microscope, using Zeiss Axiocam HR cameras and Axiovision software.

Time-lapse and still imaging

Ex vivo imaging of pigment cells in their native tissue environment followed[30,31] with images acquired at 5-min intervals for 18 hr at 10x using an Evolve (Photometrics, Tucson, AZ) camera mounted on a Zeiss Observer Z1 inverted microscope with CSU- X1 spinning disk (Yokogawa, Tokyo, Japan). Bright-field images were taken before and after imaging. Larvae were 7.5 SSL except where indicated. For analyses of *aox5*+ airinemes across stages, genetic backgrounds or both, labeled cells were examined in 79 wild-type zebrafish and 40 wild- type pearl; 4 *opallus*, 4 *ltk*, 10 *mitfa*, and 21 *cx41.8* mutants; 11 *Tg(hsp70:csf1a-DrIRES-nlsCFP)*, 4 *Tg(hsp70:kitlga)*, 5 *Tg(aox5:Tet:dnCdc42)*, 7 *Tg(tg:nVenus-2a-nfnB)* zebrafish and 13 *Tg(tg:nVenus-2a- nfnB)*

pearl; 8 ML141-treated, 4 blebbistatin-treated, 4 nocodazole-treated, 3 DMSO control zebra-fish.

Cell counts and staging

All fish were treated with epinephrine to contract pigment granules before imaging; counts were performed manually using the Cell Counter plugin feature in ImageJ. Color channel splitting and color balance modifications were used to facilitate visualization and counting of xanthophores.

Cell transplantation

Chimeric fish were generated by transplanting cells at blastula stages then rearing embryos reared through adult pigment pattern formation[24,25] using fish that were transgenic for ubiquitous *ubb:mCherry* or *actb1:EGFP*, xanthophore-lineage *aox5*:membrane-GFP, or both.

Image and statistical analyses

Digital images were color-balanced in Adobe Photoshop and adjusted for contrast and brightness; corresponding adjustments were made for images of both control and experimental fish. For repeated image series, images on consecutive days were rescaled and aligned by eye in Adobe Photoshop to control for overall growth during post- embryonic development. Statistical analyses were performed with JMP 8.0 (SAS Institute, Cary, NC). Frequency data for behaviors of individual cells or projections were assessed by single or multiple factor maximum likelihood. Contin- uous data were evaluated by *t*-test or analyses of variance, using ln-transformation in some instances to correct residuals to normality and homoscedasticity. Post hoc means were compared by Tukey- Kramer HSD.

Figure Legends

Figure 1

Evolution of cellular interactions during pigment pattern formation

(A) Zebrafish and pearl danio. Right, melanophores and xanthophores (arrows) after epinephrine treatment to contract pigment granules (**B)** Working model for pigment cell interactions during stripe development in zebrafish. In zebrafish, xanthoblasts in stripe regions extend airinemes that signal to melanophores (Xb→M), promoting their clearance from the interstripe during stripe consolidation. Additionally, iridophores have attractive and repulsive effects on melanophores (I→M; I-l M)[4,5] and express Csf1, promoting the differentiation of xanthophores (I→Xb; Xb→X)[4]. Differentiated xanthophores repel melanophores (X-l M) during normal development[7] and are capable of repressing iridophore organization (X-l I). Scale bars: 5 mm (A, left); 50μm (A, right).

Figure 2

Hypothyroid pearl danio pigment cell phenotypes

(A) Thyroid ablated pearl danio lack most hypodermal xanthophores, but retain extrahypodermal xanthophores. **(B)** Quantification of differences in hypodermal pigment cell numbers (all $P<0.0001$; imaged at 19-27 SL[26]; DMSO, $N=8$; Mtz, $N=13$). Scale bars: 100μm (A).

Figure 3

Airineme projections in zebrafish and pearl danio

(A) Long projections by zebrafish *aox5*+ cells of xanthophore lineage (arrows) with membranous vesicles (arrowhead, inset). **(B)** Zebrafish *aox5*+ cells were more likely to extend airinemes that pearl, especially during stripe development (7-8 SSL[26]); species x stage,

χ2=103.4, d.f.=4, p<0.0001; N=929, 1259 cells for zebrafish and pearl; projections per cell: χ2=45.3, d.f.=1, p<0.0001. **(C)** Extension and retraction (arrow) and release of vesicle (arrowhead) in zebrafish but not pearl as shown in these time lapse movies. (**D)** Interstripe melanophores persisted when airinemes were blocked with a pharmacological agent[6]. Cell states are indicated by logos in lower left corners (X, *aox5*+ xanthophore lineage). Insets, brownish melanophores persisting from embryonic/early larval pattern and gray-black adult melanophores. All zebrafish data collected by DSE in[6]. Scale bars: 10μm (A); 50μm (C); 200μm (D)

Figure 4

Factors extrinsic to the *aox5*+ cells inhibit airineme production and signaling in pearl

(A) Left, pearl *aox5*+ cells extended more airinemes when differentiation-arrested (TH-; χ^2=12.5, d.f.=1, p<0.0005, *N*=412 cells). Right, zebrafish *aox5*+ cells transplanted to pearl, or receiving excess Csf1 in zebrafish, extended fewer airinemes than comparably staged *aox5*+ cells in unmanipulated zebrafish (χ^2=23.1, 22.1, d.f.=1, 1; p<0.0001, *N*=846 cells total). **(B)** In chimeras resulting from transplants of zebrafish donors (*aox5:membrane-GFP,* ubiquitous *ubb:mCherry*[32]) to pearl hosts, zebrafish *aox5*+ cells (arrow) were typically intermingled with pearl melanophores, as well as *ubb*+ zebrafish melanophores (arrowheads). Scale bar: 50μm (B)

Figure 5

Models for pigment cell lineage relationships, evolution of TH-dependencies, and evolution of airineme signaling

(A) TH has a major role in adult xanthophore differentiation (1) and proliferation (2). TH also promotes the survival (3) and differentiation (4) of melanophore precursors, while simultaneously repressing the survival (5) and proliferation (6) of melanophores. These effects may be direct or mediated through other cell types or TH-dependent endocrine factors. In pearl

danio, still unidentified TH-independent factors (?) are likely to promote the differentiation of extra-hypodermal xanthophores and some hypodermal xanthophores, reducing the TH-dependence of this cell lineage. **(B)** Working models for pigment cell interactions and pattern formation in zebrafish (left) and pearl danio (right). In zebrafish, xanthoblasts in stripe regions extend airinemes that signal to melanophores (Xb→M), promoting their clearance from the interstripe during stripe consolidation. In addition to xanthoblasts-melanophore interactions, iridophores have attractive and repulsive effects on melanophores (I→M; I-l M)[4,33]. Differentiated xanthophores repel melanophores (X-l M) during normal development[7] and are capable of repressing iridophore organization (X-l I)[20]. In pearl danio, Csf1 is expressed at elevated levels by cells other than iridophores and this drives earlier and broader xanthophore differentiation than in zebrafish[20]. Precocious, widespread differentiation of xanthophores likely limits directional cues available to melanophores while simultaneously curtailing the potential for airineme signaling, as airineme competent xanthoblasts are depleted. Tissue contexts (lower panels(also show eventual death of some melanophores remaining in the interstripe in zebrafish[22,34] and the higher overall incidence of melanophore death in pearl danio[27]; iridophores are omitted for clarity.

Figure S1

Interspecific chimeras reveal non-autonomous effects on pattern and *aox5*+ cell behaviors

(A) In zebrafish→ pearl chimeras, well-organized stripes of zebrafish cells formed but only when all three classes of zebrafish pigment cells (inset: x, xanthophore; m, melanophore; i, iridophores) were present and near other zebrafish tissues (blue outline, donor myotomes). Ten adult chimeras analyzed. **(B)** In pearl→albino zebrafish chimeras (in which host melanophores were present but unpigmented), pearl melanophores were confined to stripes, adopting a zebrafish-like arrangement; stripe-interstripe boundaries are indicated by dashed white lines

and interstripes by yellow-orange bars at left. **(C)** Pearl *aox5*+ cells frequently developed in zebrafish hosts at embryonic/early larval stages (*N*=90 *aox5*+ chimeras), yet these same cells typically died prior to time-lapse imaging during adult pigment pattern formation, here apparently by fragmentation and extrusion of GFP+ debris, typical of pigment cell death in zebrafish[35,36]. **(D)** Prior to extrusion, rare, surviving pearl danio *aox5*+ cells could extend numerous airinemes in zebrafish hosts (3 airinemes are shown; *, *aox5*+ cell fragmenting during imaging). Scale bars: 100μm (A, for A and B); 20μm (C); 50μm (D).

Figure S2

Hypothyroid phenotypes in pearl danio

(A) Juvenile hypothyroid fish (Mtz-treated at 4dpf) were smaller than controls (DMSO) and had fragile fins prone to damage (arrowhead); this fin fragility was also observed in hypothyroid zebrafish. **(B)** Failure of swimbladder secondary lobe formation (outlined) and delayed scale development (arrowhead). **(C)** In thyroid-intact pearl danio, xanthophores are widespread and intermingled with melanophores (inset; arrowhead, evolutionarily reduced interstripe). In thyroid-ablated juveniles, melanophores were more abundant and xanthophores were fewer, though in contrast to zebrafish some xanthophores persisted, particularly in the residual interstripe (insets). **(D)** Thyroid-ablated fish also had altered head shapes, lacked barbels (arrowhead) and frequently had cardiac edema (arrow), also seen in hypothyroid zebrafish.

References

1. Engeszer, R., Ryan, M. & Parichy, D. Learned social preference in zebrafish. *Curr. Biol.* **14,** 881–884 (2004).
2. Engeszer, R. E., Wang, G., Ryan, M. J. & Parichy, D. M. Sex-specific perceptual spaces for a vertebrate basal social aggregative behavior. *Proc. Natl. Acad. Sci. U. S. A.* **105,** 929–33 (2008).
3. Seehausen, O. *et al.* Speciation through sensory drive in cichlid fish. *Nature* **455,** 620–626 (2008).
4. Patterson, L. B. & Parichy, D. M. Interactions with Iridophores and the Tissue Environment Required for Patterning Melanophores and Xanthophores during Zebrafish Adult Pigment Stripe Formation. *PLoS Genet.* **9,** e1003561 (2013).
5. Frohnhöfer, H. G., Krauss, J., Maischein, H.-M. & Nüsslein-Volhard, C. Iridophores and their interactions with other chromatophores are required for stripe formation in zebrafish. *Development* **140,** 2997–3007 (2013).
6. Eom, D. S., Bain, E. J., Patterson, L. B., Grout, M. E. & Parichy, D. M. Long-distance communication by specialized cellular projections during pigment pattern development and evolution. **4,** (2015).
7. Nakamasu, A., Takahashi, G., Kanbe, A. & Kondo, S. Interactions between zebrafish pigment cells responsible for the generation of Turing patterns. *Proc. Natl. Acad. Sci.* **106,** 8429–8434 (2009).
8. Maderspacher, F. Formation of the adult pigment pattern in zebrafish requires leopard and obelix dependent cell interactions. *Development* **130,** 3447–3457 (2003).
9. Lang, M. R., Patterson, L. B., Gordon, T. N., Johnson, S. L. & Parichy, D. M. Basonuclin-2 requirements for zebrafish adult pigment pattern development and female fertility. *PLoS Genet.* **5,** (2009).
10. Mcmenamin, S. K. *et al.* Thyroid hormone-dependent adult pigment cell lineage and pattern in zebrafish. *Science* **130,** 1358–1362 (2014).
11. McCluskey, B. M. & Postlethwait, J. H. Phylogeny of zebrafish, a 'model species,' within Danio, a 'model genus'. *Mol. Biol. Evol.* **32,** 635–652 (2015).
12. Fang, F., Norén, M., Liao, T. Y., Källersjö, M. & Kullander, S. O. Molecular phylogenetic interrelationships of the south Asian cyprinid genera Danio, Devario and Microrasbora (Teleostei, Cyprinidae, Danioninae). *Zool. Scr.* **38,** 237–256 (2009).
13. Vliet, G. Van & Polak, M. Thyroid Gland Development and Function. (2007).
14. Laudet, V. The origins and evolution of vertebrate metamorphosis. *Curr. Biol.* **21,** R726–R737 (2011).
15. Shi, Y. B. *Amphibian Metamorphosis from Morphology to Molecular Biology*. (Wiley-Liss, 2000).
16. McMenamin, S. K. & Parichy, D. M. *Metamorphosis in Teleosts*. *Current Topics in Developmental Biology* **103,** (Elsevier Inc., 2013).
17. van der Ven, L., van den Brandhof, E., Vos, J., Power, D. M. & Wester, P. W. Effects of the antithyroid agent propylthiouracil in a partial life cycle assay with zebrafish. *Env. Sci Technol* **40,** 74–81 (2006).
18. Curado, S., Stainier, D. Y. R. & Anderson, R. M. Nitroreductase-mediated cell/tissue ablation in zebrafish: a spatially and temporally controlled ablation method with applications in developmental and regeneration studies. *Nat. Protoc.* **3,** 948–54 (2008).
19. Hébrant, A., Van Staveren, W. C. G., Maenhaut, C., Dumont, J. E. & Leclère, J. Genetic hyperthyroidism: Hyperthyroidism due to activating TSHR mutations. *Eur. J. Endocrinol.* **164,** 1–9 (2011).
20. Patterson, L. B., Bain, E. J. & Parichy, D. M. Pigment cell interactions and differential xanthophore recruitment underlying zebrafish stripe reiteration and Danio pattern evolution. *Nat. Commun.* **5,** 1–7 (2014).

21. Parichy, D. M. *et al.* Mutational analysis of endothelin receptor b1 (rose) during neural crest and pigment pattern development in the zebrafish Danio rerio. *Dev. Biol.* **227,** 294–306 (2000).
22. Parichy, D. M. & Turner, J. M. Zebrafish puma mutant decouples pigment pattern and somatic metamorphosis. *Dev. Biol.* **256,** 242–257 (2003).
23. Takahashi, G. & Kondo, S. Melanophores in the stripes of adult zebrafish do not have the nature to gather, but disperse when they have the space to move. *Pigment Cell Melanoma Res.* **21,** 677–86 (2008).
24. Parichy, D. M. & Turner, J. M. Temporal and cellular requirements for Fms signaling during zebrafish adult pigment pattern development. *Development* **130,** 817–833 (2003).
25. Quigley, I. K. *et al.* Pigment pattern evolution by differential deployment of neural crest and post-embryonic melanophore lineages in Danio fishes. *Development* **131,** 6053–69 (2004).
26. Parichy, D. M., Elizondo, M. R., Mills, M. G., Gordon, T. N. & Engeszer, R. E. Normal table of postembryonic zebrafish development: staging by externally visible anatomy of the living fish. *Dev. Dyn.* **238,** 2975–3015 (2009).
27. Quigley, I. K. *et al.* Evolutionary diversification of pigment pattern in Danio fishes: differential fms dependence and stripe loss in D. albolineatus. *Development* **132,** 89–104 (2005).
28. Kwan, K. *et al.* The Tol2kit: a multisite gateway-based construction kit for Tol2 transposon transgenesis constructs. *Dev. Dyn.* **236,** 3088–99 (2007).
29. Urasaki, A., Morvan, G. & Kawakami, K. Functional Dissection of the Tol2 Transposable Element Identified the Minimal cis-Sequence and a Highly Repetitive Sequence in the Subterminal Region Essential for Transposition. *Genetics* **174,** 639 LP-649 (2006).
30. Budi, E. H., Patterson, L. B. & Parichy, D. M. Post-embryonic nerve-associated precursors to adult pigment cells: genetic requirements and dynamics of morphogenesis and differentiation. *PLoS Genet.* **7,** e1002044 (2011).
31. Eom, D. S. *et al.* Melanophore migration and survival during zebrafish adult pigment stripe development require the immunoglobulin superfamily adhesion molecule Igsf11. *PLoS Genet.* **8,** e1002899 (2012).
32. Mosimann, C. *et al.* Ubiquitous transgene expression and Cre-based recombination driven by the ubiquitin promoter in zebrafish. *Development* **138,** 169–177 (2011).
33. Frohnhofer, H. G., Krauss, J., Maischein, H.-M. & Nusslein-Volhard, C. Iridophores and their interactions with other chromatophores are required for stripe formation in zebrafish. *Development* **140,** 2997–3007 (2013).
34. Parichy, D. M., Ransom, D. G., Paw, B., Zon, L. I. & Johnson, S. L. An orthologue of the kit-related gene fms is required for development of neural crest-derived xanthophores and a subpopulation of adult melanocytes in the zebrafish, Danio rerio. *Development* **127,** 3031–44 (2000).
35. Lang, M. R., Patterson, L. B., Gordon, T. N., Johnson, S. L. & Parichy, D. M. Basonuclin-2 requirements for zebrafish adult pigment pattern development and female fertility. *PLoS Genet.* **5,** e1000744 (2009).
36. Parichy, D. M., Rawls, J. F., Pratt, S. J., Whitfield, T. T. & Johnson, S. L. Zebrafish sparse corresponds to an orthologue of c-kit and is required for the morphogenesis of a subpopulation of melanocytes, but is not essential for hematopoiesis or primordial germ cell development. *Development* **126,** 3425–36 (1999).

Figure 1

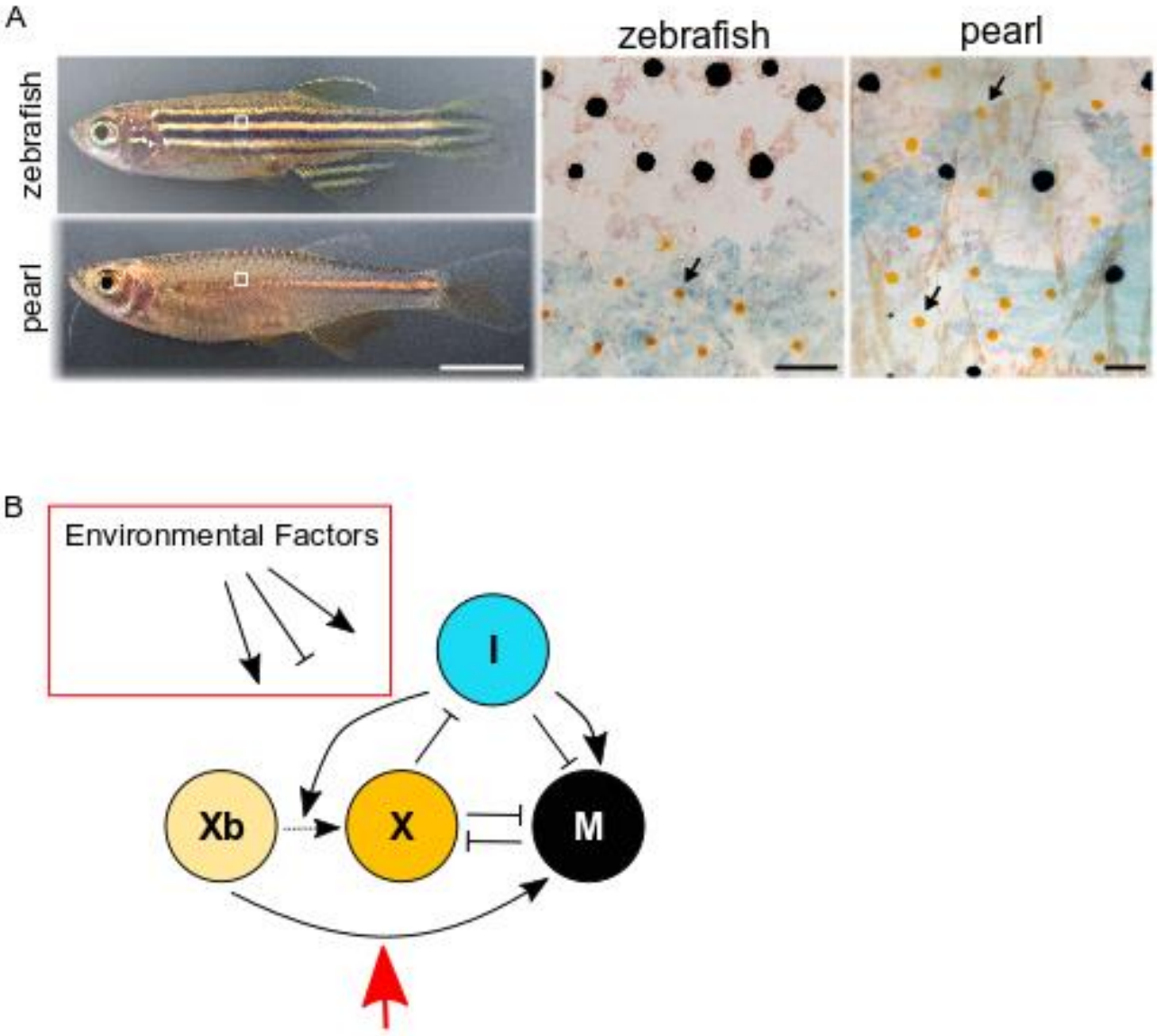
A
zebrafish
pearl
zebrafish
pearl
B
Environmental Factors
I
Xb
X
M

Figure 2

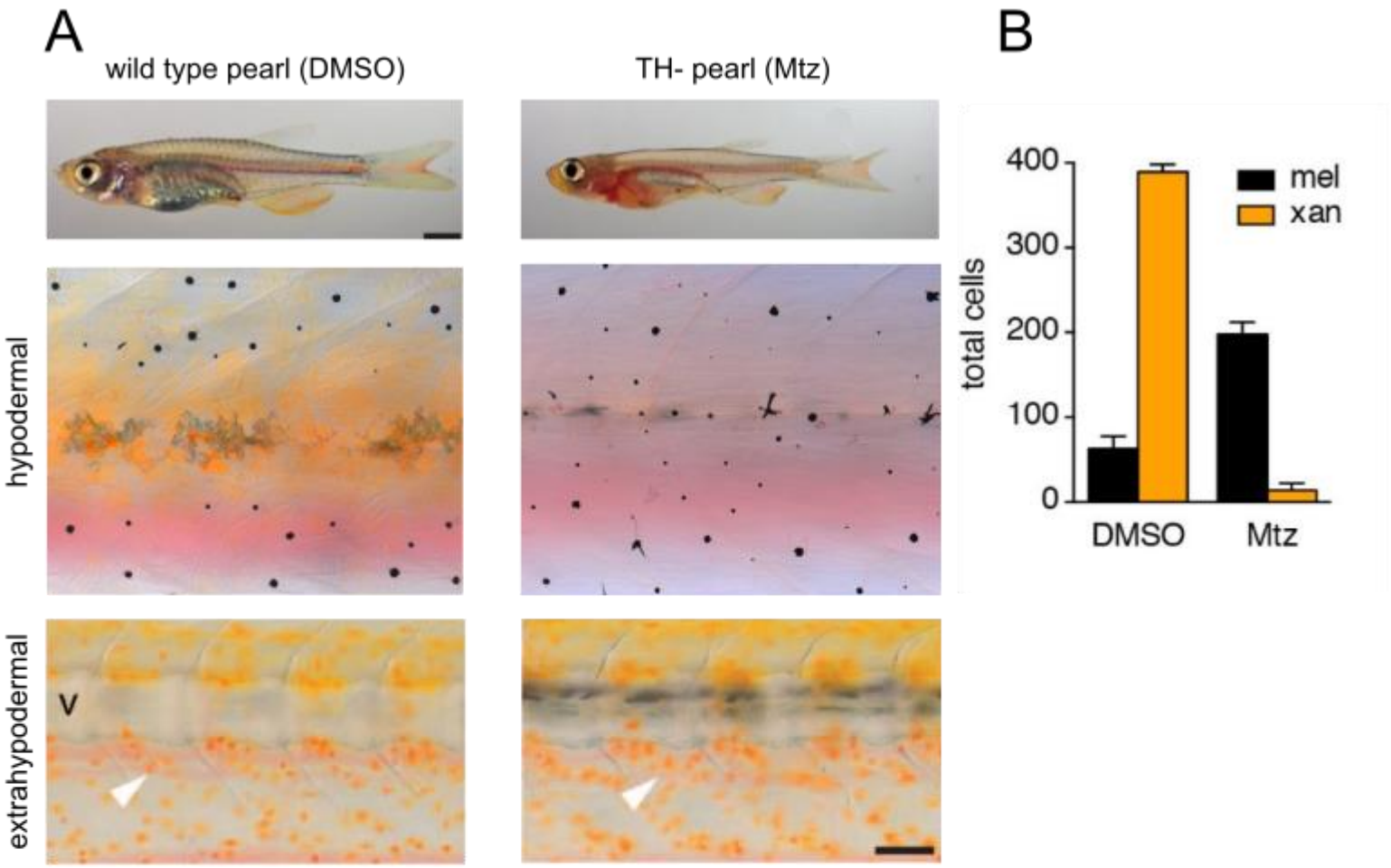
A
wild type pearl (DMSO)
TH- pearl (Mtz)
hypodermal
extrahypodermal
V
B
total cells
400
300
200
100
0
mel
xan
DMSO
Mtz

Figure 3

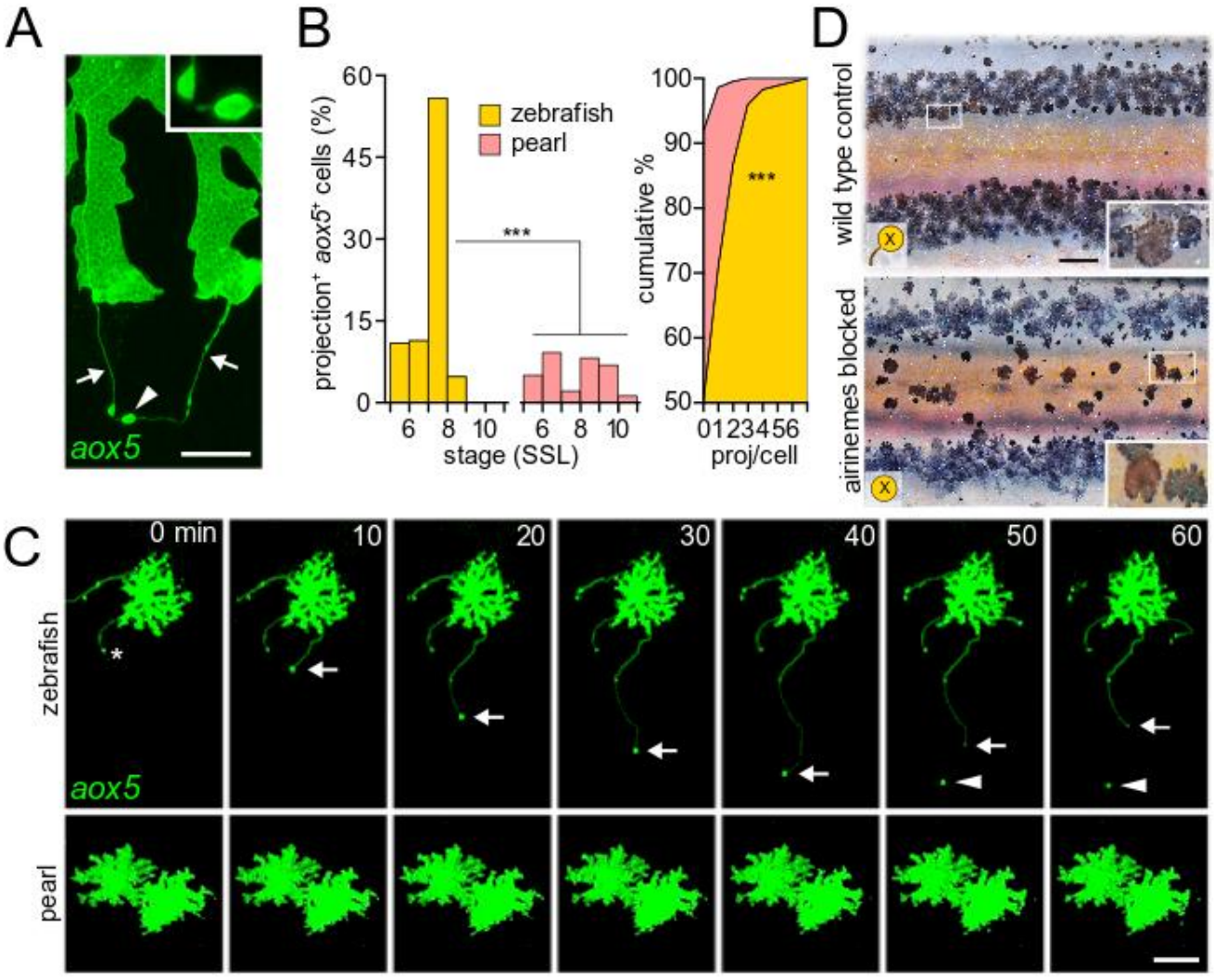
A
aox5
B
projection+ aox5+ cells (%)
zebrafish
pearl
***
stage (SSL)
cumulative %
proj/cell
D
wild type control
airinemes blocked
C
0 min
10
20
30
40
50
60
zebrafish
aox5
pearl

Figure 4

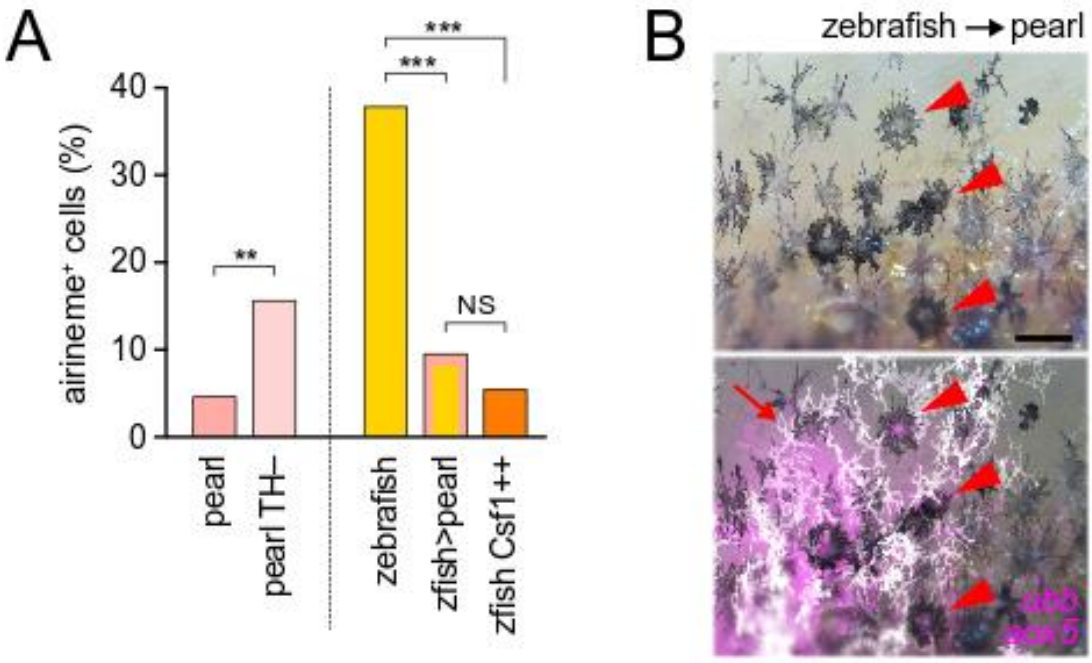
A
airineme+ cells (%)
40
30
20
10
0
**
***
***
NS
pearl
pearl TH–
zebrafish
zfish>pearl
zfish Csf1++
B
zebrafish → pearl

Figure 5

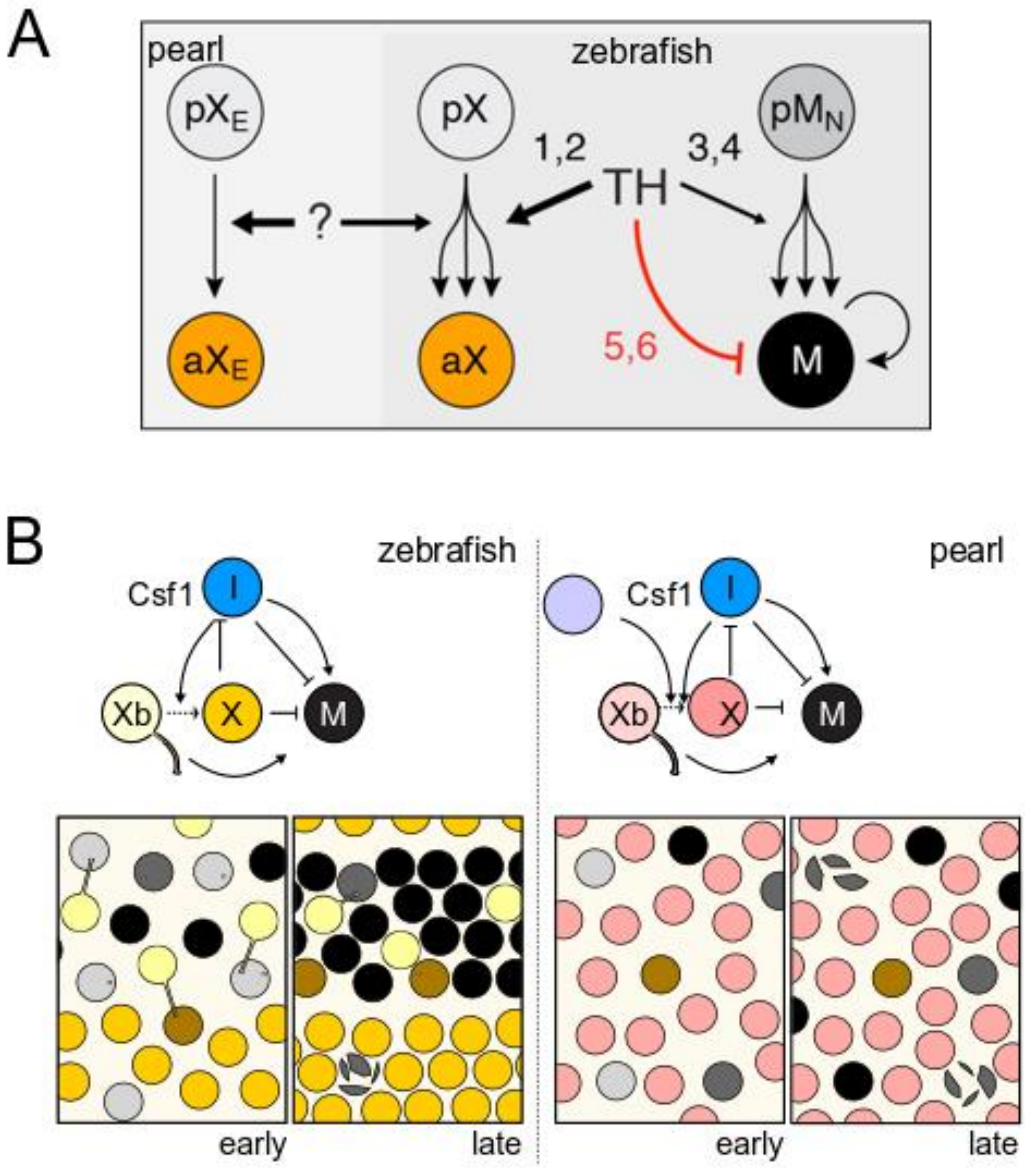
A
pearl
zebrafish
pX_E
pX
pM_N
1,2
3,4
TH
?
aX_E
aX
5,6
M
B
zebrafish
pearl
Csf1
I
Xb
X
M
early
late

Figure S1

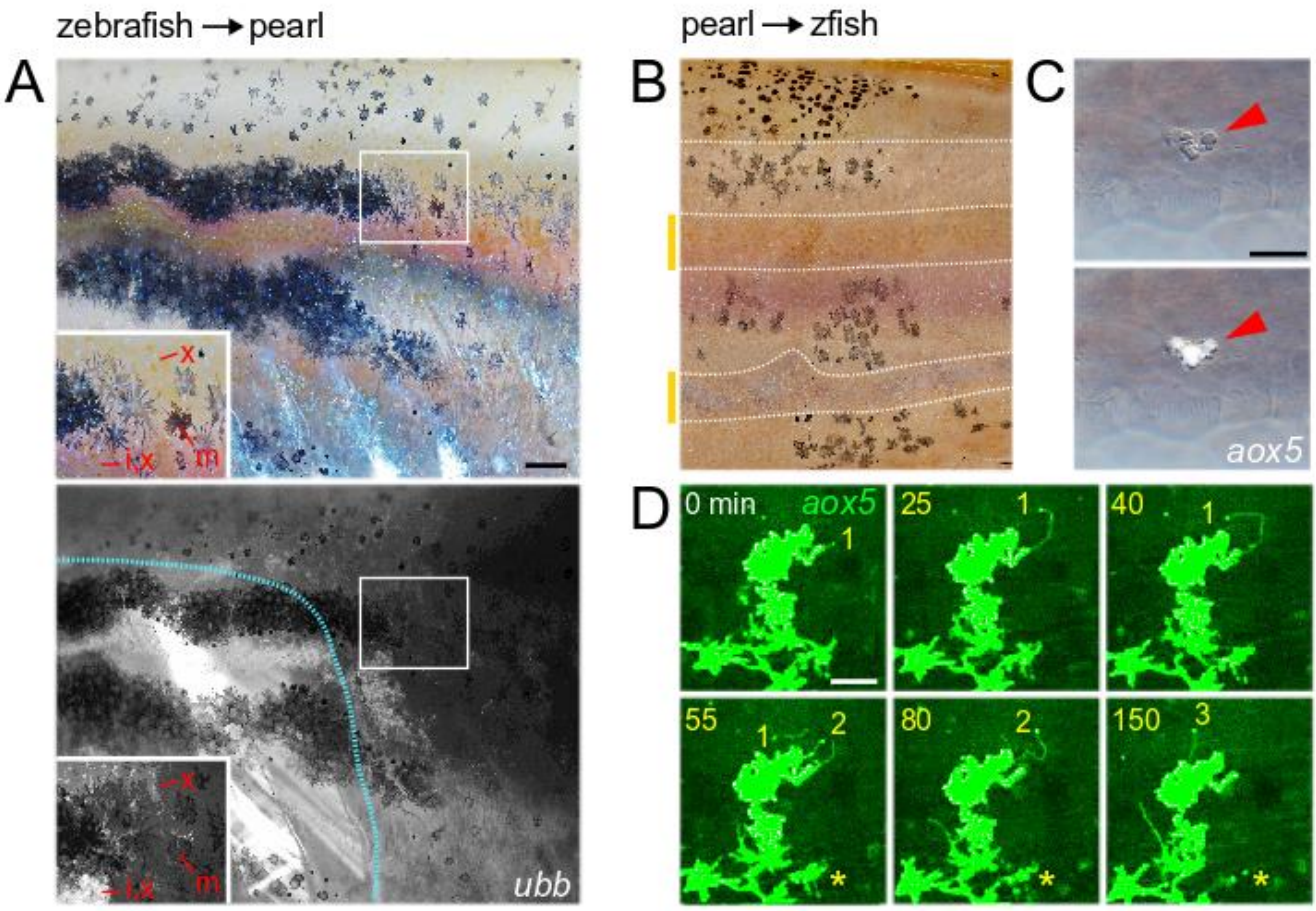
zebrafish → pearl
A
x
l
m
ubb
pearl → zfish
B
C
aox5
D
0 min
aox5
25
40
55
80
150

Figure S2